# Role of the inhomogeneity angle in anisotropic attenuation analysis

Jyoti Behura & Ilya Tsvankin
*Center for Wave Phenomena, Geophysics Department, Colorado School of Mines, Golden, Colorado 80401*

**ABSTRACT**

The inhomogeneity angle (the angle between the real and imaginary parts of the wave vector) is seldom taken into account in estimating attenuation coefficients from seismic data. Wave propagation through the subsurface, however, can result in relatively large inhomogeneity angles $\xi$, especially for models with significant attenuation contrasts across layer boundaries. Here, we study the influence of the angle $\xi$ on phase and group attenuation in arbitrarily anisotropic media using the first-order perturbation theory verified by exact numerical modeling.

Application of the spectral-ratio method to transmitted or reflected waves yields the normalized group attenuation coefficient $\mathcal{A}_g$, which is responsible for the amplitude decay along seismic rays. Our analytic solutions show that for a wide range of inhomogeneity angles the coefficient $\mathcal{A}_g$ is close to the normalized *phase* attenuation coefficient $\mathcal{A}$ computed for $\xi = 0^\circ$ ($\mathcal{A}|_{\xi=0^\circ}$). The coefficient $\mathcal{A}|_{\xi=0^\circ}$ can be inverted directly for the attenuation-anisotropy parameters, so no knowledge of the inhomogeneity angle is required for attenuation analysis of seismic data. This conclusion remains valid even for uncommonly high attenuation with the quality factor $Q$ less than 10 and strong velocity and attenuation anisotropy. However, the relationship between the group and phase attenuation coefficients becomes more complicated for relatively large inhomogeneity angles approaching so-called "forbidden directions." We also demonstrate that the velocity function remains practically independent of attenuation for a wide range of small and moderate angles $\xi$.

In principle, estimation of the attenuation-anisotropy parameters from the coefficient $\mathcal{A}|_{\xi=0^\circ}$ requires computation of the phase angle, which depends on the anisotropic velocity field. For moderately anisotropic models, however, the difference between the phase and group directions should not significantly distort the results of attenuation analysis.

## Introduction

In attenuative media, the direction of maximum attenuation of a plane wave can differ from the propagation direction. This implies that the real part of the wave vector $\mathbf{k}^R$ ("propagation vector") deviates from the imaginary part $\mathbf{k}^I$ ("attenuation vector"), as illustrated in Figure 1. The angle between the vectors $\mathbf{k}^R$ and $\mathbf{k}^I$ is called the "inhomogeneity angle," denoted here by $\xi$. When $\xi = 0^\circ$, the plane wave is often characterized as "homogeneous;" when $\xi \neq 0^\circ$, it is called "inhomogeneous." For plane-wave propagation, $\xi$ represents a free parameter except for certain "forbidden directions" (Krebes & Le, 1994; Carcione & Cavallini, 1995; Červený & Pšenčík, 2005a,b) where solutions of the wave equation do not exist. If the wavefield is excited by a point source, the inhomogeneity angle is determined by the medium properties including the boundary conditions (Zhu, 2006; Vavryčuk, 2007).

Alternatively, the wave vector in attenuative media can be parameterized in terms of the "inhomogeneity parameter" $D$ (Boulanger & Hayes, 1993; Declercq *et al.*, 2005; Červený & Pšenčík, 2005a):

$$\mathbf{k} = \omega(\sigma\mathbf{n} + iD\mathbf{m})\,, \tag{1}$$

such that

$$\mathbf{m}\cdot\mathbf{n} = 0\,, \tag{2}$$

where $D$ is real, while $\sigma$ is complex. The vector $\mathbf{n}$ specifies the direction of wave propagation, while the vector $\mathbf{m}$ is orthogonal to it. The main advantage of this parameterization is that it eliminates forbidden directions from the solutions of the Christoffel equation (Červený & Pšenčík, 2005a).

Many results on attenuation analysis are obtained under the assumption that the inhomogeneity angle can be ignored (Hauge, 1981; Dasgupta & Clark, 1998; Zhu *et al.*, 2007). For point-source radiation in homogeneous media, the influence of the inhomogeneity angle is indeed small, unless the medium is anomalously attenuative and anisotropic (Zhu, 2006; Vavryčuk, 2007).

During wave propagation in layered media, however, the angle $\xi$ can attain significant values. For the model in Figure 2, the wave vector in the elastic cap rock is real, while that in the attenuative reservoir is complex. Because the projections of the incident (real) and transmitted (complex) wave vectors onto the interface have to be the same according to Snell's law, the imaginary part $\mathbf{k}^I$ of the wave vector in the reservoir is orthogonal to the interface. This implies that the inhomogeneity angle of the transmitted wave is equal to the transmission angle, which can reach 90°. It is also clear that the inhomogeneity angle of the wave reflected from the base of the reservoir can be large as well. This situation, for example, is always encountered in soft absorbing sediments beneath the ocean bottom.

Existing measurements of the inhomogeneity angle are limited to laboratory studies (Deschamps & Assouline, 2000; Huang *et al.*, 1994). Indeed, although the angle $\xi$ can be significant, its estimation from seismic data is extremely difficult. It seems natural to expect that the inhomogeneity angle should influence the attenuation along the raypath (group attenuation), which is the only relevant attenuation measurement in seismic processing.

Attenuation analysis becomes particularly involved in anisotropic media where the ray may significantly deviate from both the phase direction and the direction of maximum attenuation. When the medium is anisotropic, the relationship between the angle $\xi$ and the attenuation coefficients is obscured by the complexity of the exact equations. It can be inferred from the work of Gajewski & Pšenčík (1992) that in weakly attenuative media the group attenuation coefficient yields the quality factor of the medium. Numerical modeling by Deschamps & Assouline (2000) also shows that group attenuation reflects the intrinsic viscoelasticity of the material. The analytic results of Vavryčuk (2008) and Červený & Pšenčík (2008a) indicate that group attenuation is insensitive to the inhomogeneity parameter. Their asymptotic analysis, however, is valid only for weak attenuation and plane waves with small values of the inhomogeneity parameter $D$.

Here, we use first-order perturbation theory to study the influence of the inhomogeneity angle on the group and phase attenuation coefficients. By perturbing an isotropic attenuative background, we obtain a weakly anisotropic medium with angular dependence of both velocity and attenuation. In contrast to the methodology of Červený & Pšenčík (2008a) and Vavryčuk (2008), our approach allows for arbitrarily large attenuation and "strongly inhomogeneous" waves. Therefore, this perturbation scheme helps us to analyze wave propagation for a wide range of angles $\xi$ including the vicinity of forbidden directions. First, we develop closed-form linearized expressions for group and phase attenuation in arbitrarily anisotropic media, which provide useful physical insight into the influence of the angle $\xi$. The general equations are then simplified for the special case of TI media by expressing them through the Thomsen-style anisotropy parameters. Finally, the conclusions drawn from the analytic expressions are corroborated by exact numerical modeling.

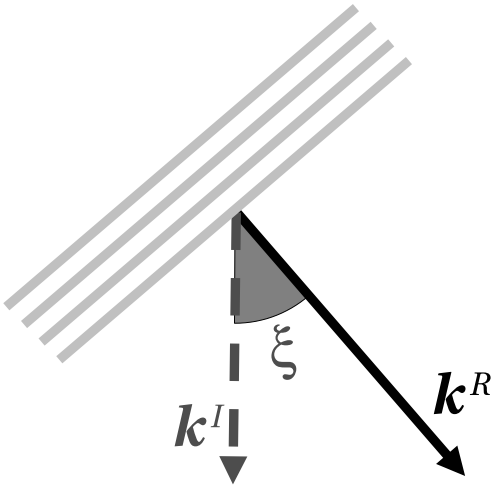


**Figure 1.** Plane wave with a nonzero inhomogeneity angle $\xi$. The wave propagates in the direction $\mathbf{k}^R$ (perpendicular to the planes of constant phase) and attenuates most rapidly in the direction $\mathbf{k}^I$.

## 1 PHASE AND GROUP ATTENUATION COEFFICIENTS

The Christoffel equation, which describes plane-wave propagation in anisotropic media, can be solved for the real ($k^R$) and imaginary ($k^I$) parts of the wave vector. The ratio $k^I/k^R$ yields the phase attenuation per wavelength, which is called the normalized phase attenuation coefficient $\mathcal{A}$ (Zhu & Tsvankin, 2006):

$$\mathcal{A} = \frac{k^I}{k^R}. \tag{3}$$

For a nonzero inhomogeneity angle $\xi$, the coefficient $\mathcal{A}$ is a measure of attenuation along the vector $\mathbf{k}^I$ rather than $\mathbf{k}^R$. Also, in seismic data processing, the attenua-

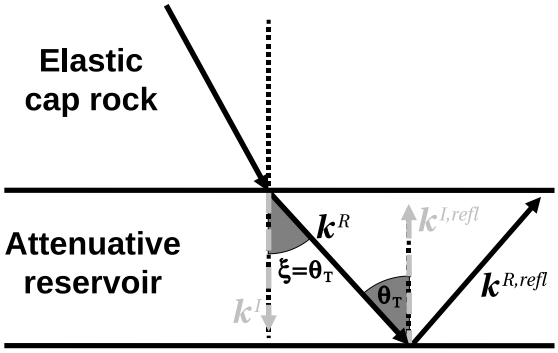


**Figure 2.** Illustration of the reflection/transmission problem at the interface between a purely elastic cap rock and an attenuative reservoir. $\mathbf{k}^R$ and $\mathbf{k}^I$ are the real and imaginary parts of the wave vector of the transmitted wave, while $\mathbf{k}^{R,refl}$ and $\mathbf{k}^{I,refl}$ correspond to the reflected wave. As discussed in the text, the inhomogeneity angle $\xi$ of the transmitted wave is equal to the transmission angle $\theta_T$.

tion is measured along the raypath, which deviates from the phase direction $\mathbf{k}^R$ when the medium is anisotropic.

Attenuation is commonly computed from seismic data using the spectral-ratio method (e.g., Johnston & Toksöz, 1981; Tonn, 1991), which has been extended to anisotropic media (Zhu *et al.*, 2007). If two receivers record the same event at two different locations along a raypath, the attenuation coefficient can be estimated from the ratio $S$ of the measured amplitude spectra:

$$\ln S = \ln \mathcal{G} - k_g^I \, l, \tag{4}$$

where $\mathcal{G}$ contains the reflection/transmission coefficients, source/receiver radiation patterns, and geometrical spreading along the raypath, $k_g^I$ is the average group attenuation coefficient, and $l$ is the distance between the two receivers. Assuming that the medium between the receivers is homogeneous, equation 4 can be rewritten in terms of the group velocity $V_g$ and traveltime $t$:

$$\ln S = \ln \mathcal{G} - k_g^I \, V_g \, t,$$

$$= \ln \mathcal{G} - \omega \, \mathcal{A}_g \, t, \tag{5}$$

where $\omega$ is the angular frequency and $\mathcal{A}_g = k_g^I / k_g^R = k_g^I / (\omega / V_g)$ is the normalized group attenuation coefficient. It follows from equation 5 that by estimating the slope of $\ln S$ expressed as a function of $\omega$, we can compute the group attenuation along the raypath, if the traveltime $t$ is known. Therefore, $\mathcal{A}_g$ is the measure of attenuation obtained from seismic data.

If the medium is anisotropic (or isotropic, but the inhomogeneity angle is large, as discussed below), the group-velocity vector $\mathbf{V}_g$ deviates from the phase direction parallel to $\mathbf{k}^R$. To simplify the analytic development, we choose a coordinate frame in which $\mathbf{k}^R$ coincides with the axis $x_3$ and $\mathbf{k}^I$ is confined to the $[x_1, x_3]$-plane (Figure 3). The group attenuation coefficient $k_g^I$ can be found by projecting the phase attenuation vector $\mathbf{k}^I$ onto the group direction:

$$k_g^I = \frac{1}{V_g} \left( \mathbf{k}^I \cdot \mathbf{V}_g \right), \tag{6}$$

$$= k^I (\cos\xi \cos\psi + \sin\xi \sin\psi \cos\phi), \tag{7}$$

where $\psi$ is the angle between $\mathbf{k}^R$ and $\mathbf{V}_g$ (group angle) and $\phi$ is the azimuth of $\mathbf{V}_g$ with respect to the $[x_1, x_3]$-plane (Figure 3). If the vectors $\mathbf{V}_g$, $\mathbf{k}^R$, and $\mathbf{k}^I$ lie in the same plane (i.e., $\phi = 0$), $k_g^I$ is given by

$$k_g^I = k^I \cos(\xi - \psi). \tag{8}$$

Using equation 7, the normalized group attenuation coefficient $\mathcal{A}_g$ can be represented as

$$\mathcal{A}_g = \frac{k_g^I}{k_g^R} = \frac{k^I \cos\xi \cos\psi \, (1 + \tan\xi \tan\psi \cos\phi)}{\omega / V_g}. \tag{9}$$

The group velocity can be obtained from the well-known relation (e.g., Červený & Pšenčík, 2006):

$$\frac{1}{\omega} \, \mathbf{k}^R \cdot \mathbf{V}_g = 1, \tag{10}$$

or

$$\frac{\omega}{V_g} = k^R \cos\psi. \tag{11}$$

Substituting equation 11 into equation 9 yields

$$\mathcal{A}_g = \frac{k^I}{k^R} \, \cos\xi \, (1 + \tan\xi \tan\psi \cos\phi). \tag{12}$$

Equation 12 can be used to compute the exact coefficient $\mathcal{A}_g$ for arbitrarily anisotropic, attenuative media and any angle $\xi$. If the group-velocity vector is confined to the plane formed by $\mathbf{k}^R$ and $\mathbf{k}^I$ (see above), $\cos\phi = 1$ and equation 12 becomes

$$\mathcal{A}_g = \frac{k^I}{k^R} \, \frac{\cos(\xi - \psi)}{\cos\psi}. \tag{13}$$

For a zero inhomogeneity angle, the coefficient $\mathcal{A}_g$ reduces to

$$\mathcal{A}_g(\xi = 0^\circ) = \left. \frac{k^I}{k^R} \right|_{\xi = 0^\circ} = \mathcal{A}|_{\xi = 0^\circ}. \tag{14}$$

Equation 14 demonstrates that even for arbitrary anisotropy, the group attenuation coefficient coincides with the phase attenuation coefficient for $\xi = 0^\circ$ (Zhu, 2006). It is unclear, however, how $\mathcal{A}_g$ is related to phase attenuation for a nonzero $\xi$ and what role is played by the inhomogeneity angle in the estimation of the attenuation coefficient.

## 2 ISOTROPIC MEDIA

To evaluate the influence of the inhomogeneity angle on velocity and attenuation in isotropic media, we obtain the real and imaginary parts of the vector $\mathbf{k}$ from the

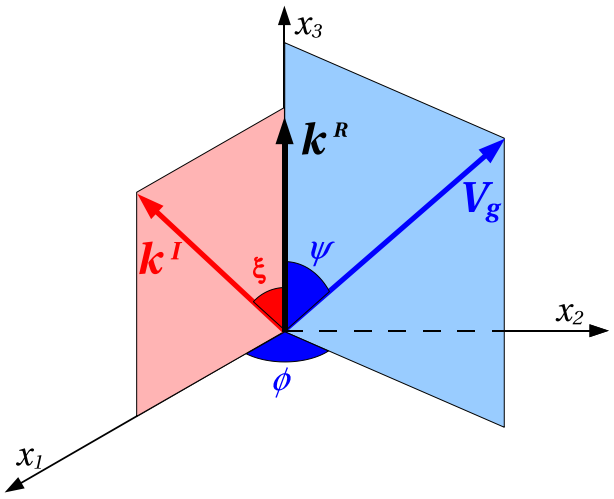


**Figure 3.** Plane wave propagating along the coordinate axis $x_3$ in an anisotropic attenuative medium. The group angle $\psi$ is the deviation of the group velocity vector $\mathbf{V}_g$ from the real part $\mathbf{k}^R$ of the wave vector. The azimuth of the vector $\mathbf{V}_g$ with respect to the plane formed by $\mathbf{k}^R$ and $\mathbf{k}^I$ is denoted by $\phi$.

wave equation. The derivation, discussed in Appendix A, shows that the solution exists only if $\mathbf{k}^R \cdot \mathbf{k}^I > 0$, which means that the inhomogeneity angle in isotropic media should be smaller than 90° (we assume that $\xi > 0$ because positive and negative inhomogeneity angles are equivalent in the absence of anisotropy). Therefore, the attenuation vector $\mathbf{k}^I$ cannot deviate from $\mathbf{k}^R$ by 90° or more, and angles $\xi \geq 90°$ correspond to so-called "forbidden directions." Note that for isotropic *non-attenuative* media, the inhomogeneity angle of an evanescent (inhomogeneous) plane wave is always equal to 90°, which explains the properties of surface and non-geometrical modes (Tsvankin, 1995).

The squared magnitudes of the vectors $\mathbf{k}^R$ and $\mathbf{k}^I$ for $\xi < 90°$ (Appendix A) are given by

$$(k^R)^2 = \frac{\omega^2}{2V^2}\left[\sqrt{1+\frac{1}{(Q\cos\xi)^2}}+1\right], \tag{15}$$

$$(k^I)^2 = \frac{\omega^2}{2V^2}\left[\sqrt{1+\frac{1}{(Q\cos\xi)^2}}-1\right], \tag{16}$$

where $V = \sqrt{a_{33}^R}$ is the real part of the medium velocity and $a_{ij}$ is the density-normalized stiffness tensor. The only approximation used to derive equations 15 and 16 is that quadratic and higher-order terms in the inverse quality factor $1/Q$ [but not in $1/(Q\cos\xi)$] can be neglected compared to unity. Equivalent solutions for $k^R$ and $k^I$ in isotropic media are given in Červený & Pšenčík (2005a).

### 2.1 Small and moderate inhomogeneity angles

The dependence of the wave vector on the inhomogeneity angle is controlled by the product $Q\cos\xi$. If the angle $\xi$ is not close to 90° and the medium does not have uncommonly strong attenuation, we can assume that $(Q\cos\xi) \gg 1$ and simplify equations 15 and 16 to (see Appendix A)

$$k^R = \frac{\omega}{V}, \tag{17}$$

$$k^I = \frac{\omega}{2VQ\cos\xi}. \tag{18}$$

According to equation 17, for $(Q\cos\xi) \gg 1$ the velocity of wave propagation is equal to $V$ and is independent of the inhomogeneity angle and of attenuation. Using equations 17 and 18, we find the normalized phase attenuation coefficient $\mathcal{A}$ as

$$\mathcal{A} = \frac{k^I}{k^R} = \frac{1}{2Q\cos\xi}. \tag{19}$$

In general, the inhomogeneity angle also influences the group velocity and the group angle. For $(Q\cos\xi) \gg 1$, however, the influence of $\xi$ is negligible (Appendix A):

$$\tan\psi = \frac{\tan\xi}{1+2Q^2} \ll 1, \tag{20}$$

and $V_g \approx V$. The normalized group attenuation coefficient $\mathcal{A}_g$ (equation 12) then becomes

$$\mathcal{A}_g = \frac{k^I\cos\xi}{k^R}. \tag{21}$$

If the wave vector is described by equations 17 and 18, equation 21 yields

$$\mathcal{A}_g = \frac{1}{2Q} = \mathcal{A}|_{\xi=0°}. \tag{22}$$

Therefore, for a wide range of common inhomogeneity angles, the group attenuation coefficient $\mathcal{A}_g$ does not depend on the angle $\xi$ and is close to the phase attenuation coefficient $\mathcal{A}$ computed for $\xi = 0°$. Later we demonstrate that this result remains valid for much more complicated models with anisotropic velocity and attenuation functions. Equation 22 also shows that seismic attenuation measurements (i.e., the coefficient $\mathcal{A}_g$) for isotropic media provide a direct estimate of the quality factor $Q$. This conclusion applies to both P- and S-waves and a wide range of angles $\xi$ (Figure 4).

### 2.2 Large inhomogeneity angles

For large inhomogeneity angles approaching 90°, the assumption $(Q\cos\xi) \gg 1$ used to derive equations 17 and 18 is no longer satisfied. In the limit of $(Q\cos\xi) \ll 1$ ($\xi \to 90°$), equations 15 and 16 give completely different approximate solutions for the wave vector (Appendix A):

$$k^R = \frac{\omega}{V\sqrt{2Q\cos\xi}}\left(1+\frac{Q\cos\xi}{2}\right), \tag{23}$$

$$k^I = \frac{\omega}{V\sqrt{2Q\cos\xi}}\left(1 - \frac{Q\cos\xi}{2}\right). \quad (24)$$

Dropping quadratic and higher-order terms in $Q\cos\xi$, we find

$$\mathcal{A} = \frac{k^I}{k^R} = 1 - Q\cos\xi\,. \quad (25)$$

The velocity of wave propagation, determined by the denominator of the expression for $k^R$ (equation 23), is proportional to $\sqrt{Q\cos\xi}$ and goes to zero when the inhomogeneity angle approaches 90°.

When $\xi \to 90°$, the influence of the inhomogeneity angle on the group quantities $\psi$, $V_g$, and $\mathcal{A}_g$ is no longer negligible. The group angle for large inhomogeneity angles becomes (Appendix A)

$$\tan\psi = \frac{1}{Q} - \cos\xi\,. \quad (26)$$

Equation 26 demonstrates that for strong attenuation (small $Q$) the group-velocity vector deviates from the phase direction.

The coefficient $\mathcal{A}_g$ for large angles $\xi$ can be obtained by substituting equations 25 and 26 into equation 12:

$$\mathcal{A}_g = (1 - Q\cos\xi)\left[\cos\xi + \left(\frac{1}{Q} - \cos\xi\right)\sin\xi\right]. \quad (27)$$

Linearizing equation 27 in $\cos\xi$ yields

$$\mathcal{A}_g = \frac{1}{Q} - \cos\xi\,. \quad (28)$$

Equation 28 shows that the group attenuation coefficient $\mathcal{A}_g$ for large inhomogeneity angles reduces to just $\tan\psi$ (see equation 26). Therefore, whereas the real and imaginary parts of the wave vector (equations 23 and 24) become infinite as $\xi \to 90°$, the group attenuation coefficient approaches $1/Q$ and is about twice as large as $\mathcal{A}|_{\xi=0°}$ (Figure 4). Hence, for large angles $\xi$ close to 90°, seismic attenuation measurements in isotropic media *do not* provide a direct estimate of the quality factor because $\mathcal{A}_g$ rapidly increases with $\xi$ from $1/(2Q)$ to $1/Q$.

Although the presence of anisotropy makes treatment of wave propagation in attenuative media much more complicated, several key conclusions drawn above prove to be valid for models with anisotropic velocity and attenuation functions.

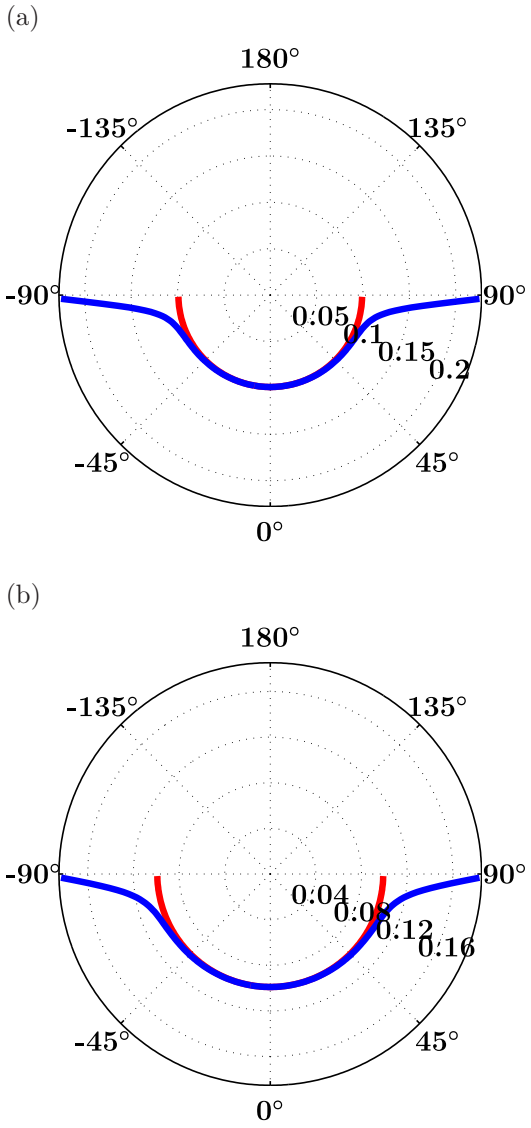


**Figure 4.** Exact P-wave (a) and S-wave (b) coefficient $\mathcal{A}|_{\xi=0°}$ (equation 3, red curve) and the normalized group attenuation $\mathcal{A}_g$ (equation 12, blue curve) in isotropic media as a function of the inhomogeneity angle $\xi$ (numbers on the perimeter). The quality factors are $Q_P = Q_S = 5$.

## 3 ANISOTROPIC MEDIA

The dependence of attenuation on the inhomogeneity angle $\xi$ in anisotropic media is influenced by the angular variation of the phase quantities and by the difference between the group and phase directions. Using the Christoffel equation B1, the phase attenuation coefficient $\mathcal{A}$ can be computed for arbitrary values of the angle $\xi$. Then general group-velocity equations (e.g., Tsvankin, 2005) can be employed to obtain the group attenuation coefficient. It would be useful, however, to develop analytic expressions for phase and group attenuation that provide physical insight into the contribution of the inhomogeneity angle. To derive analytic expressions for $\mathbf{k}^R$, $\mathbf{k}^I$, and $\mathcal{A}_g$ in arbitrarily anisotropic media, we use the first-order perturbation theory, as discussed in Appendix A. The analytic development is supported by numerical modeling based on exact solutions.

### 3.1 Perturbation of the complex wave vector

We consider an isotropic, attenuative background medium, which is perturbed to obtain anisotropic velocity and attenuation functions. The real and imaginary parts of the wave vector in the background are denoted by $\mathbf{k}^{R,0}$ and $\mathbf{k}^{I,0}$, respectively. We choose the coordinate frame in which $\mathbf{k}^{R,0}$ coincides with the $x_3$-axis and $\mathbf{k}^{I,0}$ lies in the $[x_1, x_3]$-plane. The angle $\xi$ is kept fixed, so the real and imaginary parts of the perturbed wave vector $\mathbf{k} = \mathbf{k}^R - i\mathbf{k}^I$ remain parallel to the corresponding parts of the background vector $\mathbf{k}^0$.

First, we obtain linearized expressions for the perturbations $\Delta k^R$ and $\Delta k^I$ in arbitrarily anisotropic media using the coordinate frame defined by $\mathbf{k}^R$ and $\mathbf{k}^I$ (equations B15–B20). To express $\Delta k^R$ and $\Delta k^I$ in a fixed coordinate frame, one has to rotate the perturbation density-normalized stiffness tensor $\Delta a_{ijkl}$ accordingly. For example, to derive $\Delta k^R$ and $\Delta k^I$ for TI media as a function of the phase angle $\theta$ (the angle between $\mathbf{k}^R$ and the symmetry axis), the tensor $\Delta a_{ijkl}$ in equations B15–B20 is rotated about the $x_2$-axis by the angle $\theta$.

For the special case of P-wave propagation in TI media, the perturbations $\Delta k^R$ and $\Delta k^I$ take the form

$$\frac{\Delta k_P^R}{k_P^{R,0}} = -\left(\delta \sin^2\theta\, \cos^2\theta + \epsilon \sin^4\theta\right), \tag{29}$$

$$\begin{aligned}\frac{\Delta k_P^I}{k_P^{I,0}} =& \delta_Q \sin^2\theta\, \cos^2\theta + \epsilon_Q \sin^4\theta \\ &- (\delta \sin^2\theta \cos^2\theta + \epsilon \sin^4\theta) \\ &- \left[\delta + 2(\epsilon - \delta)\sin^2\theta\right] \sin 2\theta\, \tan\xi\,,\end{aligned} \tag{30}$$

where $\epsilon$ and $\delta$ are the Thomsen velocity-anisotropy parameters, and $\epsilon_Q$ and $\delta_Q$ are the Thomsen-style attenuation-anisotropy parameters (Zhu & Tsvankin, 2006). The parameter $\epsilon_Q$ determines the fractional difference between the P-wave phase attenuation coefficients $\mathcal{A}|_{\xi=0^\circ}$ in the horizontal and vertical directions, while $\delta_Q$ controls the coefficient $\mathcal{A}|_{\xi=0^\circ}$ in the vicinity of the symmetry axis. Equations 29 and 30 are derived for the attenuation vector $\mathbf{k}^I$ confined to the plane defined by $\mathbf{k}^R$ and the symmetry axis. Similar expressions for SV- and SH-waves in TI media are given in Appendix C (equations C1–C4).

Note that the real part $\Delta k^R$ of the linearized perturbation in the wave vector in equations 29, C1, and C3 is independent of the inhomogeneity angle and is entirely governed by velocity anisotropy. This conclusion is corroborated by the numerical example in Figure 5. As the inhomogeneity angle varies from 0° to 70°, there is no noticeable change in $k^R$ even in the presence of velocity anisotropy (Figures 5c and 5d) and attenuation anisotropy (Figures 5e and 5f). The "isotropic" behavior of $k^R$ in Figures 5e and 5f indicates that attenuation anisotropy has little influence on the velocity function, which is controlled by the velocity-anisotropy parameters (Figures 5c and 5d). Whereas equations 29, C1, and C3 remain accurate for a wide range of $\xi$ (Figures 5b, 5d, and 5f) and strong attenuation anisotropy, they break down for the angle $\xi$ approaching 90°.

The attenuation vector $k^I$ (equations 30, C2, and C4), on the other hand, is influenced by both velocity and attenuation anisotropy, as well as by the inhomogeneity angle $\xi$. The increase in $\xi$ from 0° to 70° in Figure 6 causes a substantial change in $k^I$, both for isotropic and TI media. Figures 6d–6i illustrate the dependence of $k^I$ on the velocity- and attenuation-anisotropy parameters. It is interesting to note that for small $\xi$ the contribution of velocity and attenuation anisotropy to $k^I$ (equations 30, C2, and C4) is of the same order. With increasing $\xi$, however, the influence of velocity anisotropy (Figure 6f) becomes more pronounced compared to that of attenuation anisotropy (Figure 6i) because the $\tan\xi$-term in equation 30 depends just on $\epsilon$ and $\delta$. Figure 6 also demonstrates that equation 30 deviates from the exact $k^I$ only for large angles $\xi$, with the error primarily controlled by the velocity-anisotropy parameters.

### 3.2 Normalized group attenuation coefficient

As discussed above, for zero inhomogeneity angle the normalized group attenuation coefficient $\mathcal{A}_g$ coincides with $\mathcal{A}|_{\xi=0^\circ}$ (equation 14). This conclusion, which is valid for all wave modes, is supported by Figures 7a and 7b where the coefficients $\mathcal{A}|_{\xi=0^\circ}$ (red curve) and $\mathcal{A}_g$ (blue) coincide when $\xi = 0^\circ$.

To examine the influence of the angle $\xi$ on $\mathcal{A}_g$, we linearize equation 12 in terms of the perturbations of the wave vector:

$$\begin{aligned}\mathcal{A}_g &= \frac{k^{I,0} + \Delta k^I}{k^{R,0} + \Delta k^R} \cos\xi\,(1 + \tan\xi \tan\psi\cos\phi) \\ &= \frac{k^{I,0}}{k^{R,0}}\left(1 + \frac{\Delta k^I}{k^{I,0}} - \frac{\Delta k^R}{k^{R,0}}\right)\cos\xi\,(1 + \tan\xi\tan\psi\cos\phi)\,.\end{aligned} \tag{31}$$

Taking into account that $k^{I,0}/k^{R,0} = 1/(2Q^0\cos\xi)$ (equation 19), we find

$$\mathcal{A}_g = \frac{1}{2Q^0}\left(1 + \frac{\Delta k^I}{k^{I,0}} - \frac{\Delta k^R}{k^{R,0}}\right)(1 + \tan\xi\tan\psi\cos\phi). \tag{32}$$

Equation 32 is valid in arbitrarily anisotropic media for all wave modes. Substituting equations B15 and B16 for $\Delta k^R$ and $\Delta k^I$ and equation B26 for the product $\tan\psi\cos\phi$ into equation 32, we obtain the group atten-

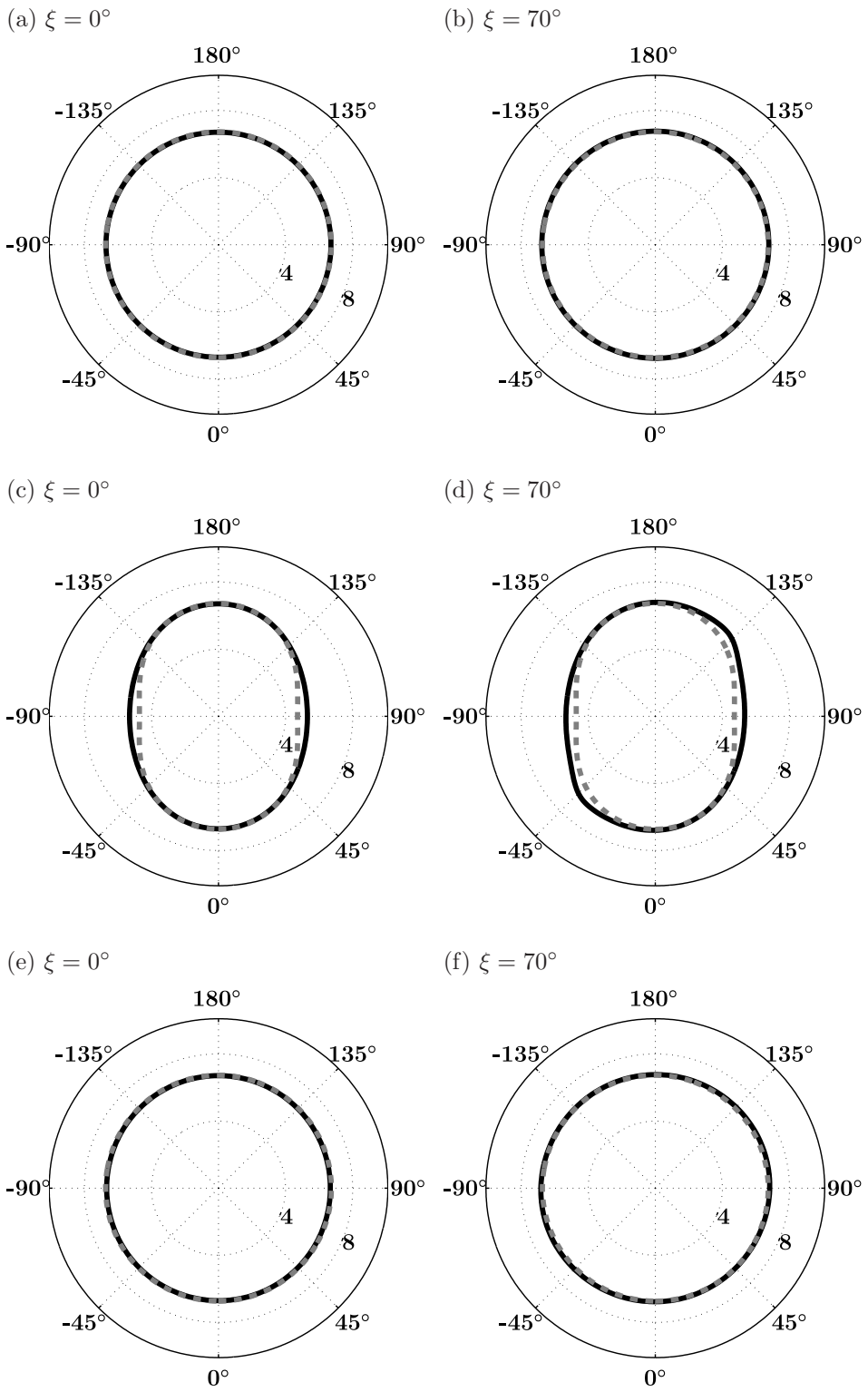


**Figure 5.** Exact real part $k^R$ (in 100 $m^{-1}$) of the P-wave vector $\mathbf{k}$ (solid lines) and approximate $k^R = k^{R,0} + \Delta k^R$ from equation 29 (dashed lines) for $\xi = 0°$ (a,c,e) and $\xi = 70°$ (b,d,f) as a function of the phase angle (numbers on the perimeter). The model in (a,b) is isotropic; in (c,d) it is anisotropic in terms of velocity but has isotropic attenuation, while in (e,f) it has isotropic velocity and anisotropic attenuation (Table 1). The frequency is 30 Hz.

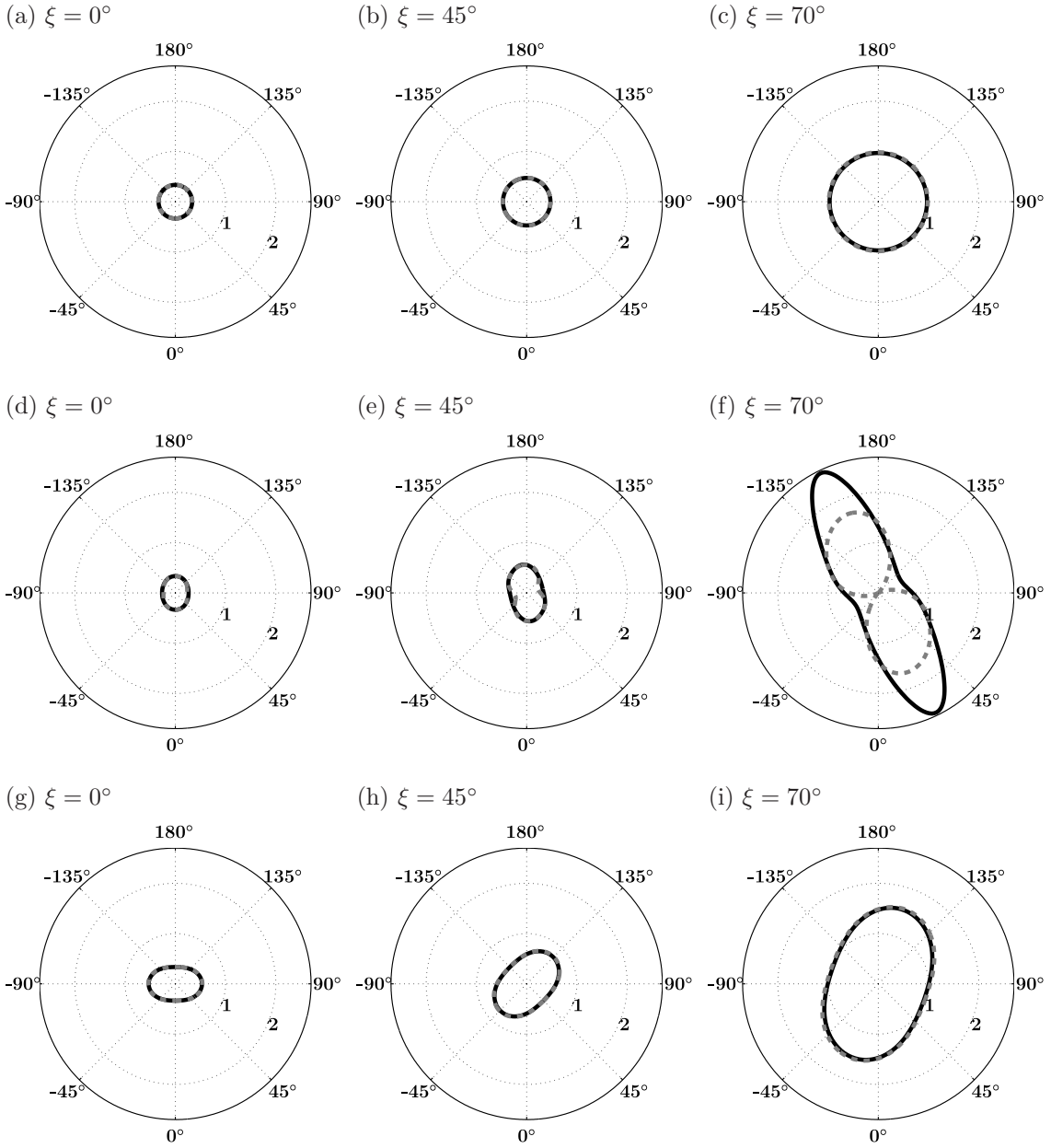


**Figure 6.** Exact imaginary part $k^I$ of the P-wave vector $\mathbf{k}$ (solid lines) and approximate $k^I = k^{I,0} + \Delta k^I$ (in 100 m$^{-1}$) from equation 30 (dashed lines) for $\xi = 0°$ (a,d,g), $\xi = 45°$ (b,e,h) and $\xi = 70°$ (c,f,i) as a function of the angle between $\mathbf{k}^I$ and the symmetry axis. In (a,b,c) both velocity and attenuation are isotropic; in (d,e,f) only velocity varies with angle, while attenuation is isotropic; in (g,h,i) attenuation varies with angle, while velocity is isotropic. The model parameters are given in Table 1. The frequency is 30 Hz.

uation coefficient for P-waves linearized in $\Delta a_{ij}$:

$$\mathcal{A}_{g,P} = \frac{1}{2Q_{P0}} - \frac{1}{2V_{P0}^2}\left(\frac{\Delta a_{33}^R}{Q_{P0}} - \Delta a_{33}^I\right), \tag{33}$$

where $Q_{P0}$ and $V_{P0}$ are the P-wave quality factor and velocity, respectively, in the background. Similar expressions for $S_1$- and $S_2$-waves are given in Appendix B (equations B30 and B31).

Below we analyze equation 33 for the special case of P-wave propagation in TI media with arbitrary symmetry-axis orientation. As mentioned earlier, to express $\mathcal{A}_g$ through the phase angle $\theta$ with the symmetry axis, the tensor $\Delta a_{ijkl}$ in equation 33 has to be rotated around the $x_2$-axis. Then we linearize $\mathcal{A}_g$ in the velocity-

| | $\xi$ | $\epsilon$ | $\delta$ | $\gamma$ | $Q_{P0}$ | $Q_{S0}$ | $\epsilon_Q$ | $\delta_Q$ | $\gamma_Q$ |
|---|---|---|---|---|---|---|---|---|---|
| Figs. 5a,b | 0°, 70° | 0 | 0 | 0 | 10 | 10 | 0 | 0 | 0 |
| 5c,d | 0°, 70° | 0.3 | 0.2 | 0 | 10 | 10 | 0 | 0 | 0 |
| 5e,f | 0°, 70° | 0 | 0 | 0 | 10 | 10 | 0.6 | 0.4 | 0 |
| Figs. 6a,b,c | 0°, 45°, 70° | Same as in Figures 5a,b | | | | | | | |
| 6d,e,f | 0°, 45°, 70° | Same as in Figures 5c,d | | | | | | | |
| 6g,h,i | 0°, 45°, 70° | Same as in Figures 5e,f | | | | | | | |
| Fig. 7a | 0° | 0.3 | 0.2 | 0 | 10 | 10 | 0.6 | 0.4 | 0 |
| 7b | 0° | 0 | 0 | 0.3 | 10 | 10 | 0 | 0 | 0.5 |
| Fig. 8 | - | 0.3 | 0.2 | 0 | 5 | 5 | 0.6 | 0.4 | 0 |
| Fig. 9a | 60° | 0 | 0 | 0 | 10 | 10 | 0 | 0 | 0 |
| 9b | 60° | 0.3 | 0.2 | 0 | 10 | 10 | 0 | 0 | 0 |
| 9c | 60° | 0.6 | 0.4 | 0 | 10 | 10 | 0 | 0 | 0 |
| 9d | 60° | 0 | 0 | 0 | 10 | 10 | 0.6 | 0.4 | 0 |
| Fig. 10a,b | 60° | 0.6 | 0.4 | 0 | 10 | 10 | 0.6 | 0.4 | 0 |
| 10c,d | 60° | 0 | 0 | 0.5 | 10 | 10 | 0 | 0 | 0.5 |
| Fig. 11 | - | 0 | 0 | 0.3 | 5 | 5 | 0 | 0 | 0.5 |
| Fig. 12a | - | 0 | 0 | 1 | 5 | 5 | 0 | 0 | -0.5 |
| 12b | - | 0 | 0 | 0.3 | 5 | 5 | 0 | 0 | -0.5 |

**Table 1.** Medium parameters used in the numerical tests. For all models, the P- and S-wave symmetry-direction velocities ($V_{P0}$ and $V_{S0}$) are 2800 m/s and 1700 m/s, respectively.

and attenuation-anisotropy parameters to obtain

$$\mathcal{A}_{g,P} = \frac{1}{2Q_{P0}} \left(1 + \delta_Q \sin^2\theta \cos^2\theta + \epsilon_Q \sin^4\theta\right). \qquad (34)$$

Similar approximate expressions for the group attenuation coefficient of SV- and SH-waves are given in Appendix C (equations C10 and C11).

Therefore, the inhomogeneity angle has no influence on the approximate group attenuation coefficient. Furthermore, $\mathcal{A}_{g,P}$ in equation 34 coincides with the linearized P-wave phase attenuation coefficient for a zero inhomogeneity angle ($\mathcal{A}|_{\xi=0^\circ}$) derived by Zhu and Tsvankin (2006). Equation 34 deviates from the exact $\mathcal{A}_g$ only when the angle $\xi$ approaches forbidden directions (Figure 8); the behavior of $\mathcal{A}_g$ for large inhomogeneity angles is analyzed in more detail below.

Note that the linearized $\mathcal{A}_g$ (equations 34, C10, and C11) is controlled by attenuation anisotropy and does not depend on the velocity-anisotropy parameters. This conclusion is confirmed by the exact modeling results in Figures 9a and 9b where the coefficient $\mathcal{A}_g$ remains insensitive even to strong velocity anisotropy with $\epsilon = 0.6$ and $\delta = 0.4$ when $\xi = 60^\circ$ (Figure 9c). The presence of attenuation anisotropy, on the other hand, results in a substantial change in $\mathcal{A}_g$ (Figure 9d).

### 3.3 Relationship between group and phase attenuation

The normalized phase attenuation coefficient $\mathcal{A}|_{\xi=0^\circ}$ can be obtained from the Christoffel equation and expressed through the attenuation-anisotropy parameters (Zhu & Tsvankin, 2006). As shown above, the coefficient $\mathcal{A}_g$ coincides with $\mathcal{A}|_{\xi=0^\circ}$ for a wide range of $\xi$ in isotropic media and for $\xi = 0^\circ$ in anisotropic media.

Using perturbation analysis, we obtained closed-form expressions for the coefficient $\mathcal{A}|_{\xi=0^\circ}$ in arbitrarily anisotropic media linearized in $\Delta a_{ij}$ (Appendix B). For P-waves,

$$\mathcal{A}|_{\xi=0^\circ,P} = \frac{1}{2Q_{P0}} - \frac{1}{2V_{P0}^2}\left(\frac{\Delta a_{33}^R}{Q_{P0}} - \Delta a_{33}^I\right). \qquad (35)$$

Similar expressions for $S_1$- and $S_2$-waves are given in Appendix B. Comparison of equations 33 and 35 shows that for a wide range of angles $\xi$ (except for values close to 90°; see below), the linearized coefficient $\mathcal{A}_g$ coincides with $\mathcal{A}|_{\xi=0^\circ}$. This conclusion is also valid for $S_1$- and $S_2$-waves (compare equations B30 and B31 with equations B24 and B25).

The approximate P-wave phase attenuation coefficient for TI media can be found as a simple function of the attenuation-anisotropy parameters (Zhu & Tsvankin, 2006):

$$\mathcal{A}|_{\xi=0^\circ,P} = \frac{1}{2Q_{P0}} \left(1 + \delta_Q \sin^2\theta \cos^2\theta + \epsilon_Q \sin^4\theta\right). \qquad (36)$$

Zhu & Tsvankin (2006) also provide similar linearized expressions for SV- and SH-waves reproduced in Appendix B. As is the case for arbitrary ansisotropy, the coefficient $\mathcal{A}|_{\xi=0^\circ}$ in equation 36 coincides with $\mathcal{A}_g$ in equation 34.

Figures 10a and 10b demonstrate that the maximum difference between the exact coefficients $\mathcal{A}_g$ and $\mathcal{A}|_{\xi=0^\circ}$ does not exceed 10% even for strong attenuation ($Q_{33} = 10$) and uncommonly large anisotropy parameters ($\epsilon = \epsilon_Q = 0.6$ and $\delta = \delta_Q = 0.4$). The coefficients $\mathcal{A}_g$ and $\mathcal{A}|_{\xi=0^\circ}$ are also close for SV- and SH-waves, which confirms the analytic results of Appendix C (Figures 10c and 10d).

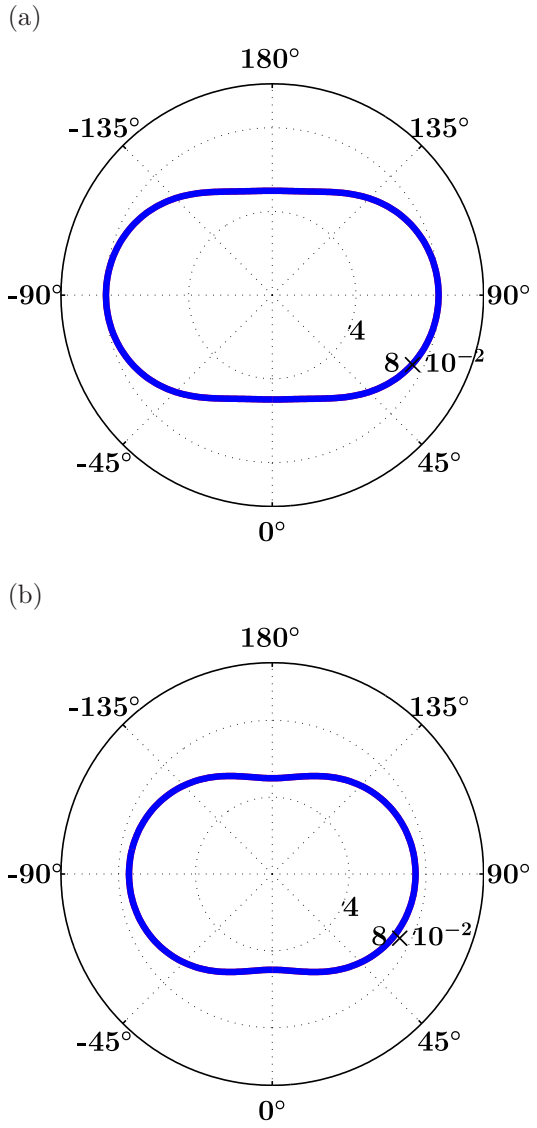


**Figure 7.** Exact P-wave (a) and SH-wave (b) coefficients $\mathcal{A}|_{\xi=0^\circ}$ (red curves) and $\mathcal{A}_g$ (blue curves) in TI media as a function of the phase angle for $\xi = 0^\circ$. Because $\mathcal{A}_g = \mathcal{A}|_{\xi=0^\circ}$, the red curves are coincident with the blue curves. The model parameters are given in Table 1.

### 3.4 Group attenuation for large inhomogeneity angles

The above conclusions about the influence of the inhomogeneity angle on phase velocity and attenuation no longer hold for large inhomogeneity angles approaching forbidden directions. As shown above for isotropic media, when $(Q\cos\xi) \ll 1$, the group attenuation coefficient varies with the angle $\xi$ and differs from $\mathcal{A}|_{\xi=0^\circ}$.

To study the influence of large $\xi$ analytically, we follow the same perturbation-based approach (Appendix B) but with different background values of the wave

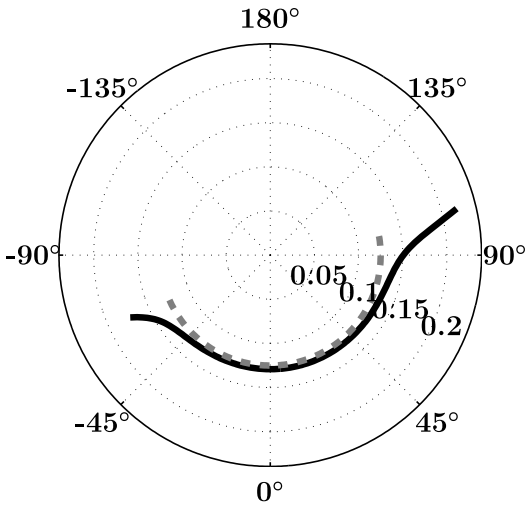


**Figure 8.** Exact P-wave group attenuation coefficient $\mathcal{A}_{g,P}$ (solid line) and approximate $\mathcal{A}_{g,P}$ from equation 34 (dashed line) in TI media for $\theta = 45^\circ$ as a function of the angle $\xi$ (numbers on the perimeter). The model parameters are given in Table 1.

vector, group velocity, and group angle (equations 23–26). For simplicity, here we analyze only the special case of elliptical anisotropy in TI media (i.e., SH-waves); more general solutions for shear waves in arbitrarily anisotropic media are given in Appendix D. Numerical tests demonstrate that our conclusions remain valid for all wave modes and any anisotropic symmetry.

According to equation D6, the coefficient $\mathcal{A}_g$ for large inhomogeneity angles becomes a function of $\xi$ and cannot serve as a measure of intrinsic attenuation. As was the case for isotropy, $\mathcal{A}_g$ in anisotropic media is always finite (and does not go to zero), even though the real and imaginary parts of the wave vector (equation D3) become infinite.

When the medium is isotropic, a physical solution of the wave equation exists only for $-90^\circ < \xi < 90^\circ$ [equation A5; also see Červený & Pšenčík (2005a)]. The bounds for the inhomogeneity angle in arbitrarily anisotropic media depend on both velocity and attenuation anisotropy and can be derived from equation D3 using the inequalities $k^R > 0$ and $k^I > 0$. For the special case of elliptical anisotropy (equation D4), the inhomogeneity angle should satisfy

$$\cos\xi + \frac{\gamma\sin 2\theta}{2}\sin\xi > \frac{\gamma_Q\cos 2\theta}{4Q_{S0}}\,, \tag{37}$$

which yields the following bounds for $\xi$:

$$-\beta - \alpha < \xi < \beta - \alpha\,, \tag{38}$$

where

$$\alpha = \tan^{-1}\left(\frac{-\gamma\sin 2\theta}{2}\right) \tag{39}$$

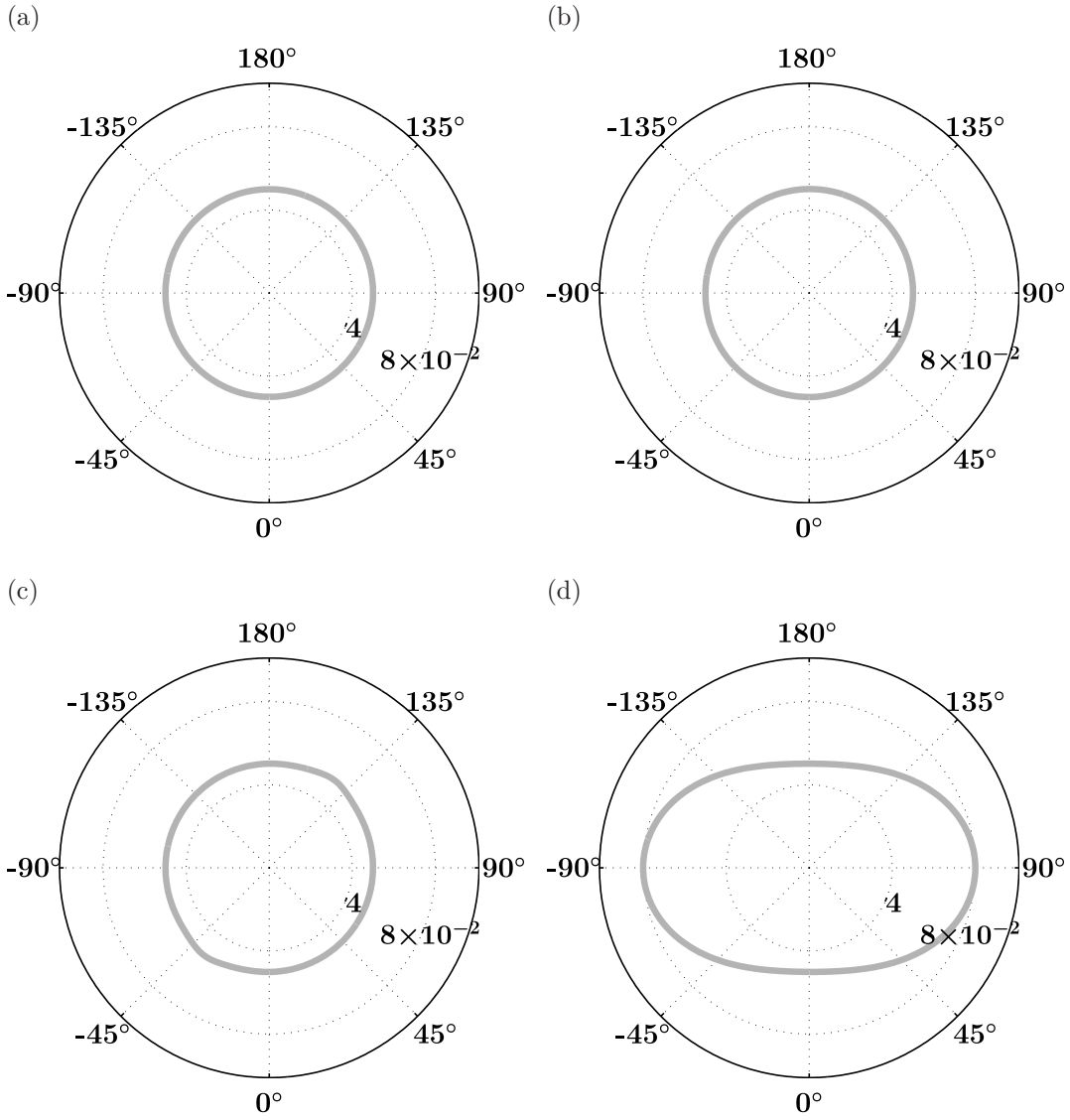


**Figure 9.** Exact P-wave group attenuation coefficient $\mathcal{A}_g$ for $\xi = 60°$ in isotropic (a) and TI (b,c,d) media. In (b,c) only velocity varies with angle, while attenuation is isotropic; in (d) attenuation varies with angle, while velocity is isotropic. The model parameters are given in Table 1.

and

$$\beta = \cos^{-1}\left(\frac{\gamma_Q \cos 2\theta}{4Q_{S0}}\right) . \tag{40}$$

Equivalent expressions for the bounds on $\xi$ for SH-wave propagation in the symmetry plane of a monoclinic medium are given by Červený & Pšenčík (2005a) in terms of the inhomogeneity parameter $D$.

For wave propagation along the symmetry axis or perpendicular to it ($\theta = 0°$ or $90°$), the angle $\alpha = 0°$ and the bounds on $\xi$ are symmetric with respect to $\xi = 0°$ (equations 38 and 40; Figure 11). It is also clear from equation 40 that $\beta \approx 90°$ because the ratio $\gamma_Q/Q_{S0}$ typically is small. Hence, for $\theta = 0°$ and $90°$ anisotropy does not signficantly change the bounds on $\xi$, which remain close to $\pm 90°$. As was the case for isotropic media, when the angle $\xi$ approaches the "forbidden directions," the group attenuation coefficient $\mathcal{A}_g$ rapidly increases with $|\xi|$ and reaches values approximately twice as large as $\mathcal{A}|_{\xi=0°}$ (Figure 11).

For oblique propagation angles, $\alpha$ does not vanish, and the bounds on $\xi$ become asymmetric with respect to $\xi = 0°$. This asymmetry is controlled by the velocity-anisotropy coefficient $\gamma$ and reaches its maximum for the phase angle $\theta = 45°$ (equation 39). The model in Figure 12a, taken from Carcione & Cavallini (1995), has an uncommonly large parameter $\gamma$ equal to unity, and for

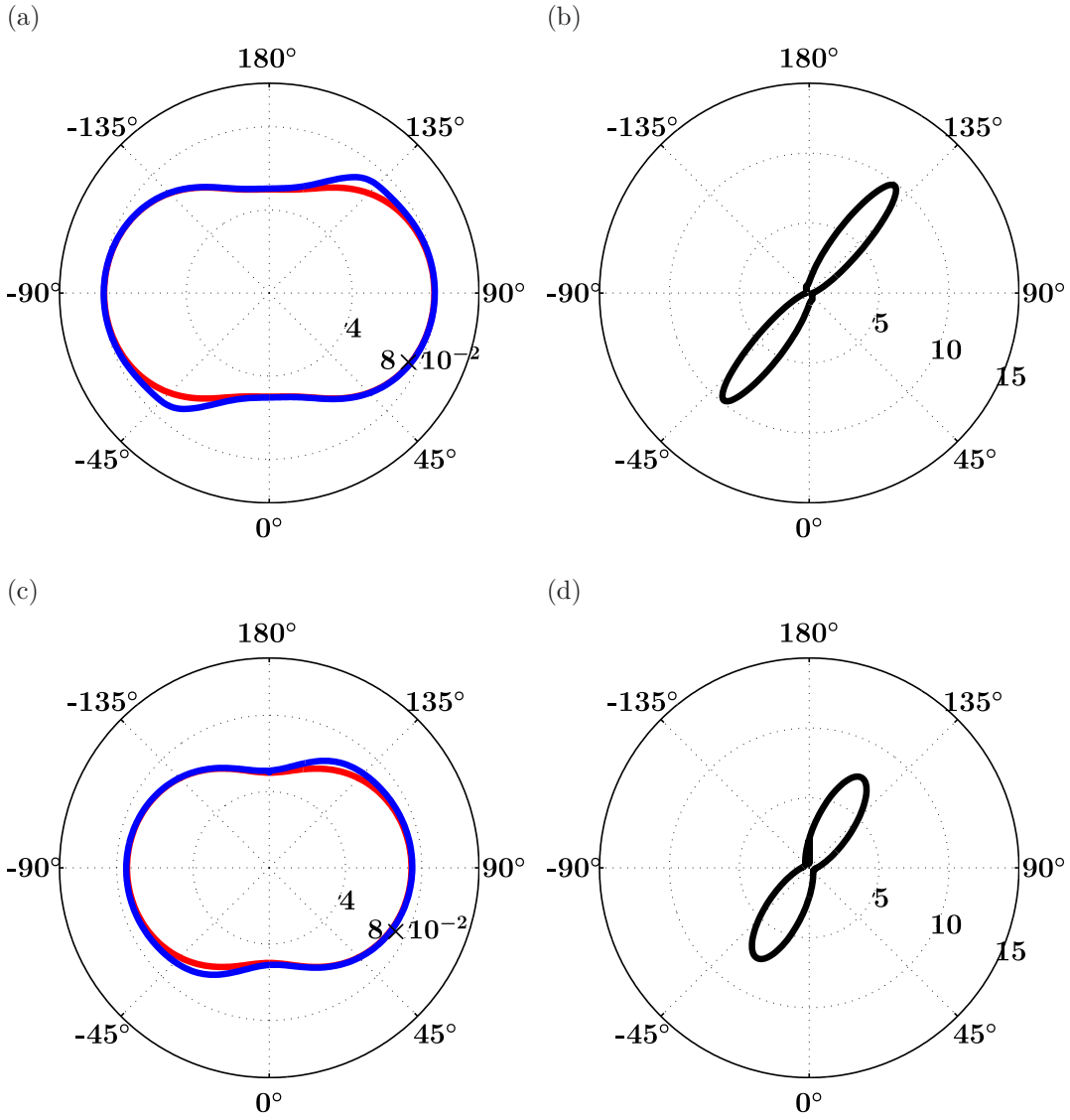


**Figure 10.** Exact P-wave (a) and SH-wave (c) coefficients $\mathcal{A}|_{\xi=0^\circ}$ (red curve) and $\mathcal{A}_g$ (blue curve) and the percentage difference $|\mathcal{A}_g - \mathcal{A}|_{\xi=0^\circ}|$ (b,d) in TI media as a function of the phase angle $\theta$ for $\xi = 60^\circ$. The model parameters are listed in Table 1.

$\theta = 45^\circ$ the inhomogeneity angle can vary between only $-64^\circ$ and $116^\circ$. Therefore, strong velocity anisotropy may result in forbidden directions for angles $|\xi|$ much smaller than $90^\circ$.

Still, the range of possible inhomogeneity angles ($2\beta$) remains close to $180^\circ$ because the parameter $\beta \approx 90^\circ$ (Figure 12a). For more common, smaller values of the parameter $\gamma$, the bounds on $\xi$ become more symmetric with respect to $\xi = 0^\circ$ and do not differ significantly from $\pm 90^\circ$ (Figure 12b). The behavior of the coefficient $\mathcal{A}_g$ for large angles $\xi$ in Figure 12 is similar to that in isotropic media.

## 4 DISCUSSION

Our analytic and numerical results for plane-wave propagation prove that the normalized group attenuation coefficient $\mathcal{A}_g$ measured from seismic data is practically independent of the inhomogeneity angle (except for angles $\xi$ approaching the forbidden directions) and is close to the normalized phase attenuation coefficient $\mathcal{A}|_{\xi=0^\circ}$. Behura & Tsvankin (2008) corroborate this conclusion by applying attenuation layer stripping and the spectral-ratio method to full-waveform P-wave synthetic data generated by a point source in layered anisotropic models. The interval coefficients $\mathcal{A}_g$ and $\mathcal{A}|_{\xi=0^\circ}$ estimated by Behura & Tsvankin (2008) from reflection am-

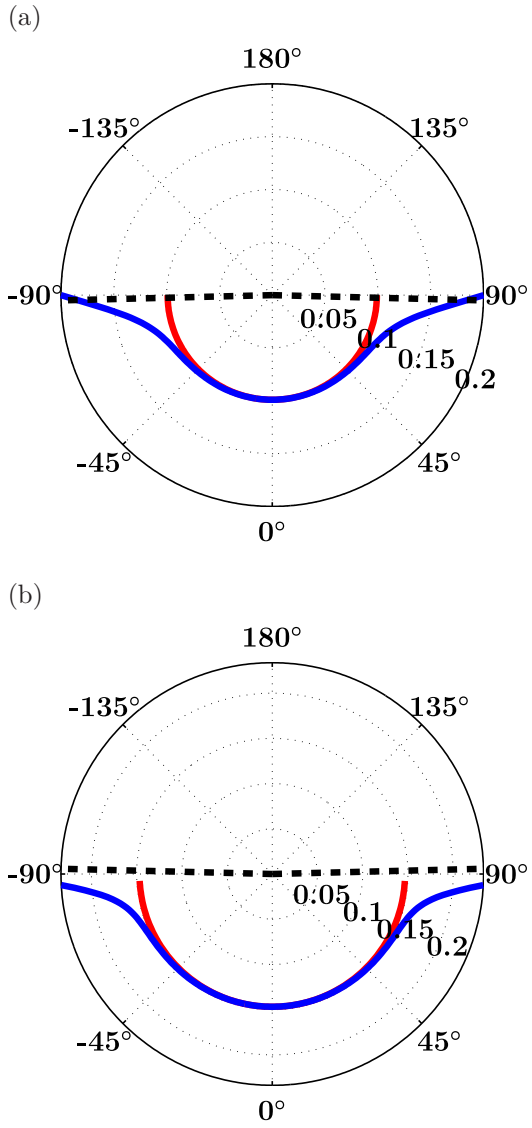


**Figure 11.** Exact SH-wave coefficients $\mathcal{A}|_{\xi=0^\circ}$ (red curve) and $\mathcal{A}_g$ (blue curve) in TI media for propagation in the directions $\theta = 0^\circ$ (a) and $\theta = 90^\circ$ (b) plotted as a function of the inhomogeneity angle $\xi$ (numbers on the perimeter). The black dashed line marks the bounds of $\xi$ computed from equations 38–40. The model parameters are listed in Table 1.

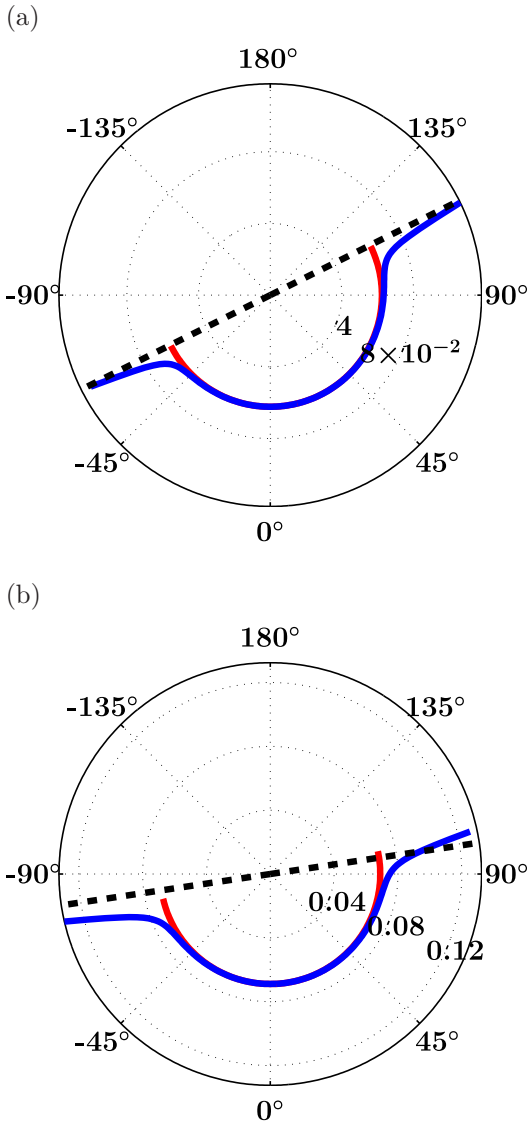


**Figure 12.** Exact SH-wave coefficients $\mathcal{A}|_{\xi=0^\circ}$ (red curve) and $\mathcal{A}_g$ (blue) as a function of $\xi$ (numbers on the perimeter) for $\theta = 45^\circ$ and $\gamma = 1.0, \gamma_Q = -0.5$ (a) and $\gamma = 0.3, \gamma_Q = -0.5$ (b). The black dashed line marks the bounds of $\xi$ computed from equations 38–40. The model parameters are listed in Table 1.

plitudes practically coincide even at large offsets where the inhomogeneity angle reaches 60°.

The coefficient $\mathcal{A}|_{\xi=0^\circ}$ in TI and orthorhombic media can be inverted for the Thomsen-style attenuation-anisotropy parameters using the formalism developed by Zhu & Tsvankin (2006, 2007). Note that estimation of the attenuation-anisotropy parameters from $\mathcal{A}|_{\xi=0^\circ}$ requires computation of the corresponding phase angle, which depends on the anisotropic velocity field. Even in strongly anisotropic models, however, the influence of attenuation on velocity is of the second order (see above), which implies that velocity analysis can be performed using existing methods. The reconstructed velocity field can then be employed to recompute the known group direction into the phase direction needed in the inversion for the attenuation-anisotropy parameters. Furthermore, given the large uncertainty of amplitude measurements, the difference between the phase and group directions for moderately anisotropic models should not significantly distort the results of attenuation analysis.

## 5 CONCLUSIONS

We applied the first-order perturbation theory to study the influence of the inhomogeneity angle on velocity and attenuation in arbitrarily anisotropic media. By adopting an attenuative, isotropic background medium, we were able to specify a background wave vector with an arbitrary inhomogeneity angle $\xi$. The perturbation analysis yields concise analytic expressions for the complex wave vector $\mathbf{k}$, the phase attenuation coefficient $\mathcal{A}|_{\xi=0^\circ}$ and the group attenuation coefficient $\mathcal{A}_g$ in terms of the perturbations of the complex stiffness coefficients. To gain physical insight into the influence of the inhomogeneity angle, we also derived closed-form expressions for TI media by linearizing the general solutions in the dimensionless velocity- and attenuation-anisotropy parameters.

For a wide range of small and moderate angles $\xi$, the phase-velocity function is practically independent of attenuation, while the group attenuation coefficient $\mathcal{A}_g$, which is measured from seismic data, is insensitive to the inhomogeneity angle. Furthermore, $\mathcal{A}_g$ practically coincides with the phase attenuation coefficient $\mathcal{A}|_{\xi=0^\circ}$, which can be treated as the angle-dependent inverse quality factor in anisotropic media. This conclusion remains valid even for uncommonly high attenuation ($Q \approx 10$) and strong velocity and attenuation anisotropy. The negligible difference between $\mathcal{A}_g$ and $\mathcal{A}|_{\xi=0^\circ}$ suggests that seismic data can be inverted for the attenuation-anisotropy parameters without knowledge of the inhomogeneity angle.

However, for larger angles $\xi$ approaching the forbidden directions (i.e., the directions of the attenuation vector $\mathbf{k}^I$ for which solutions of the wave equation do not exist) the inhomogeneity angle has a strong influence on both attenuation and phase velocity. While for isotropic media the inhomogeneity angle can vary between -90° and 90°, velocity anisotropy makes the bounds on the inhomogeneity angle asymmetric with respect to $\xi = 0^\circ$. In the vicinity of the forbidden directions the coefficient $\mathcal{A}_g$ rapidly increases with $|\xi|$ and reaches values approximately twice as large as $\mathcal{A}|_{\xi=0^\circ}$. The range of such "anomalous" inhomogeneity angles where $\mathcal{A}_g$ no longer represents a direct measure of the intrinsic attenuation becomes wider for highly attenuative models.

## ACKNOWLEDGMENTS

We are grateful to the members of the A(nisotropy)-Team of the Center for Wave Phenomena (CWP), Colorado School of Mines for helpful discussions. Support for this work was provided by the Consortium Project on Seismic Inverse Methods for Complex Structures at CWP and by the Petroleum Research Fund of the American Chemical Society.

## References

Behura, J., & Tsvankin, I. 2008. Estimation of interval anisotropic attenuation from reflection data. *SEG Technical Program Expanded Abstracts*.

Boulanger, P., & Hayes, M. A. 1993. *Bivectors and Waves in Mechanics and Optics*. 1 edn. Chapman & Hall/CRC.

Carcione, J. M., & Cavallini, F. 1995. Forbidden directions for inhomogeneous pure shear waves in dissipative anisotropic media. *Geophysics*, **60**(2), 522–530.

Červený, V., & Pšenčík, I. 2005a. Plane waves in viscoelastic anisotropic media-I. Theory. *Geophysical Journal International*, **161**, 197–212.

Červený, V., & Pšenčík, I. 2005b. Plane waves in viscoelastic anisotropic media-II. Numerical examples. *Geophysical Journal International*, **161**, 213–229.

Červený, V., & Pšenčík, I. 2006. Energy flux in viscoelastic anisotropic media. *Geophysical Journal International*, **166**(Sept.), 1299–1317.

Červený, V., & Pšenčík, I. 2008a. Quality factor Q in dissipative anisotropic media. *Geophysics*, **73**(4), T63–T75.

Červený, V., & Pšenčík, I. 2008b. Weakly inhomogeneous plane waves in anisotropic, weakly dissipative media. *Geophysical Journal International*, **172**, 663–673.

Dasgupta, R., & Clark, R. A. 1998. Estimation of Q from surface seismic reflection data. *Geophysics*, **63**(6), 2120–2128.

Declercq, N. F., Briers, R., Degrieck, J., & Leroy, O. 2005. The history and properties of ultrasonic inhomogeneous waves. *IEEE Transactions on Ultrasonics, Ferroelectrics and Frequency Control*, **52**(5), 776–791.

Deschamps, M., & Assouline, F. 2000. Attenuation Along the Poynting Vector Direction of Inhomogeneous Plane Waves in Absorbing and Anisotropic Solids. *Acta Acustica united with Acustica*, **86**, 295–302.

Gajewski, D., & Pšenčík, I. 1992. Vector wavefields for weakly attenuating anisotropic media by the ray method. *Geophysics*, **57**(1), 27–38.

Hauge, P. S. 1981. Measurements of attenuation from vertical seismic profiles. *Geophysics*, **46**(11), 1548–1558.

Huang, W., Briers, R., Rokhlin, S. I., & Leroy, O. 1994. Experimental study of inhomogeneous wave reflection from a solid–air periodically rough boundary using leaky Rayleigh waves. *The Journal of the Acoustical Society of America*, **96**(1), 363–369.

Jech, J., & Pšenčík, I. 1989. First-order perturbation method for anisotropic media. *Geophysical Journal International*, **99**(nov), 369–376.

Johnston, D. H., & Toksöz, M. N. 1981. *Seismic wave attenuation*. Geophysics reprint series, Society of Exploration Geophysicists.

Krebes, E. S., & Le, L. H. T. 1994. Inhomogeneous plane waves and cylindrical waves in anisotropic

anelastic media. *Journal of Geophysical Research*, **99**(B12), 899–919.

Tonn, R. 1991. The determination of the seismic quality factor Q from VSP data: A comparison of different computational methods. *Geophysical Prospecting*, **39**(1), 1–27.

Tsvankin, I. 1995. *Seismic Wavefields in Layered Isotropic Media*. Samizdat Press.

Tsvankin, I. 2005. *Seismic Signatures and Analysis of Reflection Data in Anisotropic Media*. 2 edn. Elsevier Science.

Vavryčuk, V. 2007. Ray velocity and ray attenuation in homogeneous anisotropic viscoelastic media. *Geophysics*, **72**(6), D119–D127.

Vavryčuk, V. 2008. Velocity, attenuation, and quality factor in anisotropic viscoelastic media: A perturbation approach. *Geophysics*, **73**(5), D63–D73.

Zhu, Y. 2006. *Seismic wave propagation in attenuative anisotropic media*. Ph.D. thesis, Colorado School of Mines.

Zhu, Y., & Tsvankin, I. 2006. Plane-wave propagation in attenuative transversely isotropic media. *Geophysics*, **71**(2), T17–T30.

Zhu, Y., & Tsvankin, I. 2007. Plane-wave attenuation anisotropy in orthorhombic media. *Geophysics*, **72**(1), D9–D19.

Zhu, Y., Tsvankin, I., Dewangan, P., & van Wijk, K. 2007. Physical modeling and analysis of P-wave attenuation anisotropy in transversely isotropic media. *Geophysics*, **72**(1), D1–D7.

## APPENDIX A: COMPLEX WAVE VECTOR FOR ISOTROPIC ATTENUATIVE MEDIA

We consider a harmonic plane wave with an arbitrary inhomogeneity angle $\xi$ propagating in isotropic attenuative media:

$$A(\mathbf{x},t) = A_0\, e^{i(\omega\, t\, -\, \mathbf{k}\cdot\mathbf{x})}\,, \tag{A1}$$

where $\omega$ is the angular frequency and $\mathbf{k} = \mathbf{k}^R - i\,\mathbf{k}^I$ is the complex wave vector responsible for the velocity and the attenuation coefficient. Substitution of the plane wave A1 into the acoustic wave equation results in

$$k_1^2 + k_2^2 + k_3^2 = \frac{\omega^2}{V^2\left(1 + \dfrac{i}{Q}\right)}\,, \tag{A2}$$

where $V$ is the real part of the medium velocity, and $Q$ is the quality factor. Dropping quadratic and higher-order terms in $1/Q$, we rewrite equation A2 as

$$(k^R)^2 - 2\,i\,\mathbf{k}^R\cdot\mathbf{k}^I - (k^I)^2 = \frac{\omega^2}{V^2}\left(1 - \frac{i}{Q}\right); \tag{A3}$$

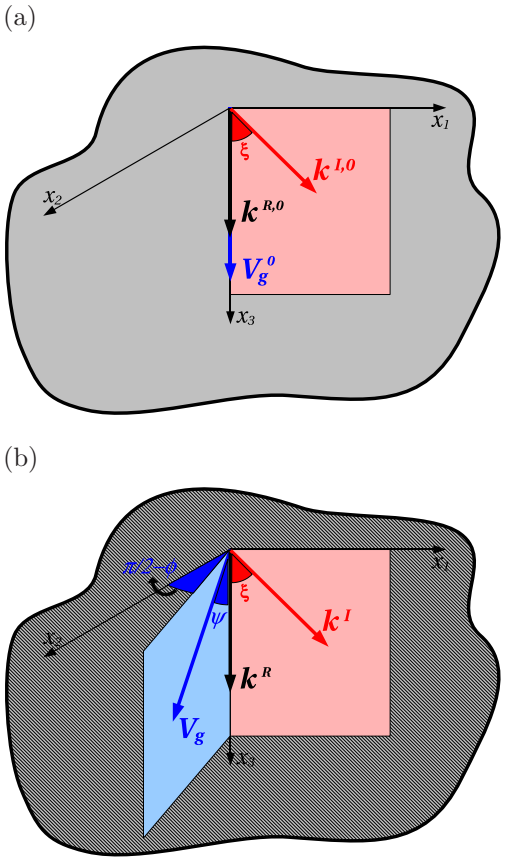


**Figure A1.** Isotropic attenuative background medium (a) is perturbed to make it anisotropic (b). $\mathbf{k}^{R,0}$ and $\mathbf{k}^{I,0}$ are the real and imaginary parts of the wave vector in the background, and $\mathbf{k}^R = \mathbf{k}^{R,0} + \Delta\mathbf{k}^R$ and $\mathbf{k}^I = \mathbf{k}^{I,0} + \Delta\mathbf{k}^I$ form the wave vector in the perturbed medium; $\xi$ is the inhomogeneity angle. The vectors $\mathbf{k}^{R,0}$ and $\mathbf{k}^R$ are parallel to the vertical $x_3$ direction while $\mathbf{k}^{I,0}$ and $\mathbf{k}^I$ are confined to the $[x_1, x_3]$-plane. $\mathbf{V}_g^0$ is the group velocity in the background; $\psi$ is the polar group angle after the perturbation, and $\phi$ is the azimuth of the perturbed vector $\mathbf{V}_g$ with respect to the $[x_1, x_3]$-plane.

$k^R = |\mathbf{k}^R|$ and $k^I = |\mathbf{k}^I|$. Equation A3 can be separated into the real and imaginary parts:

$$(k^R)^2 - (k^I)^2 = \frac{\omega^2}{V^2}\,, \tag{A4}$$

$$\mathbf{k}^R\cdot\mathbf{k}^I = \frac{\omega^2}{2V^2\,Q}\,. \tag{A5}$$

When the medium is non-attenuative and $1/Q = 0$, the right-hand side of equation A5 vanishes. Then the vectors $\mathbf{k}^R$ and $\mathbf{k}^I$ of an inhomogeneous (evanescent) plane wave have to be orthogonal, with the relationship between $k^R$ and $k^I$ determined by equation A4.

Because the factor $Q$ responsible for attenuation is positive, equation A5 can be satisfied only if $\mathbf{k}^R\cdot\mathbf{k}^I > 0$, which requires that $\cos\xi > 0$ and $\xi < 90°$. (We make

the assumption that $\xi > 0$ because the solutions of equations A4 and A5 do not depend on the sign of $\xi$.) With the inhomogeneity angle smaller than 90°, equation A5 allows us to express $k^I$ through $k^R$ as

$$k^I = \frac{\omega^2}{2\,k^R\,V^2\,Q\cos\xi}\,. \tag{A6}$$

Substitution of $k^I$ into equation A4 yields a quadratic equation for $(k^R)^2$, which has only one positive solution:

$$(k^R)^2 = \frac{\omega^2}{2V^2}\left[\sqrt{1+\frac{1}{(Q\cos\xi)^2}}+1\right]. \tag{A7}$$

The corresponding imaginary part $k^I$ can be obtained from either equation A4 or A6:

$$(k^I)^2 = \frac{\omega^2}{2V^2}\left[\sqrt{1+\frac{1}{(Q\cos\xi)^2}}-1\right]. \tag{A8}$$

For typical large values of the quality factor, the product $(Q\cos\xi) \gg 1$, unless the inhomogeneity angle is close to 90°. Expanding the radical in equations A7 and A8 in $1/(Q\cos\xi)^2$, we find

$$k^R \cong \frac{\omega}{V}\left[1+\frac{1}{8(Q\cos\xi)^2}\right], \tag{A9}$$

$$k^I \cong \frac{\omega}{2VQ\cos\xi}\left[1-\frac{1}{8(Q\cos\xi)^2}\right]. \tag{A10}$$

Equations A9 and A10 can be simplified further by neglecting the small (compared to unity) term $1/[8(Q\,\cos\xi)^2]$:

$$k^R = \frac{\omega}{V}\,, \tag{A11}$$

$$k^I = \frac{\omega}{2VQ\cos\xi}\,. \tag{A12}$$

### A1 Large inhomogeneity angles

Although equations A11 and A12 are sufficiently accurate for a wide range of inhomogeneity angles, they break down when $\xi \to 90°$. For $(Q\cos\xi) \ll 1$, equations A7 and A8 can be approximated by

$$k^R = \frac{\omega}{V\sqrt{2Q\cos\xi}}\left(1+\frac{Q\,\cos\xi}{2}\right), \tag{A13}$$

$$k^I = \frac{\omega}{V\sqrt{2Q\cos\xi}}\left(1-\frac{Q\,\cos\xi}{2}\right). \tag{A14}$$

The phase attenuation coefficient $\mathcal{A}$ can be found from equations A13 and A14:

$$\mathcal{A} = \frac{k^I}{k^R} = 1 - Q\cos\xi\,; \tag{A15}$$

here, we have dropped the term quadratic in $(Q\cos\xi)$.

### A2 Group angle

In elastic isotropic media, the group- and phase-velocity vectors are always parallel. If, however, the medium is strongly attenuative and $\xi \neq 0°$, the group direction might deviate from the phase direction. The group-velocity vector in arbitrarily anisotropic, attenuative media can be computed from (Červený & Pšenčík, 2006)

$$(V_g)_i = \frac{S_i}{\mathbf{S}\cdot\mathbf{p}^R}$$

$$= \frac{(a_{ijkl}\,g_k\,g_j^*\,p_l)^R}{(a_{ijkl}\,g_k\,g_i^*\,p_l)^R\,p_j^R}\,, \tag{A16}$$

where $\mathbf{S}$ is the energy flux, $a_{ijkl}$ is the density-normalized stiffness tensor, $\mathbf{p}$ is the slowness vector, and $\mathbf{g}$ is the polarization vector; the superscripts "$R$" and "$*$" represent the real part and complex conjugate, respectively.

For isotropic media, equation A16 yields the following components of $\mathbf{V}_g$:

$$\mathbf{V}_g = \frac{\omega}{k^R}\left[\frac{k^I\sin\xi}{k^RQ+k^I\cos\xi},\,0,\,1\right]. \tag{A17}$$

From equation A17, we find the group angle $\psi$:

$$\tan\psi = \frac{k^I\sin\xi}{k^R\,Q+k^I\cos\xi}\,. \tag{A18}$$

To obtain the group angle for small and moderate inhomogeneity angles, we substitute equations A11 and A12 into equation A18, yielding

$$\tan\psi = \frac{\tan\xi}{1+2Q^2} \ll 1\,. \tag{A19}$$

For angles $\xi$ approaching 90°, we substitute equation A15 into equation A18 and linearize the result in $\cos\xi$ to get

$$\tan\psi = \frac{1}{Q} - \cos\xi\,. \tag{A20}$$

It is clear that for large inhomogeneity angles and strongly attenuative media, the angle $\psi$ may not be negligible.

## APPENDIX B: PERTURBATION ANALYSIS

Here, we derive analytic expressions for the real and imaginary parts of the wave vector in arbitrarily anisotropic, attenuative media using first-order perturbation theory. A homogeneous, isotropic, attenuative full space is taken as the background medium (Figure A1a). The inhomogeneity angle $\xi$ between the real $(k^{R,0})$ and imaginary $(k^{I,0})$ parts of the wave vector in the background can be arbitrarily large. The background medium is perturbed to make it anisotropic in terms of both velocity and attenuation (Figure A1b), which results in perturbations of the real $(\Delta k^R)$ and

imaginary ($\Delta k^I$) parts of the wave vector. Because the inhomogeneity angle $\xi$ is a free parameter, we choose not to perturb it when making the medium anisotropic. This implies that the vectors $\mathbf{k}^R$ and $\mathbf{k}^{R,0}$, as well as $\mathbf{k}^I$ and $\mathbf{k}^{I,0}$, are parallel.

We choose $\mathbf{k}^0$ such that $\mathbf{k}^{R,0}$ coincides with the axis $x_3$ and $\mathbf{k}^{I,0}$ lies in the $[x_1, x_3]$-plane (Figures A1a and A1b). This approach differs from the one adopted by Jech & Pšenčík (1989), Červený & Pšenčík (2008b), and Vavryčuk (2008), who used a fixed reference frame. To compute the perturbations for a different vector $\mathbf{k}$ in the same medium, we rotate the coordinate frame such that $\mathbf{k}^R$ coincides with the axis $x_3$ and $\mathbf{k}^I$ lies in the $[x_1, x_3]$-plane. This approach involves the rotation of the density-normalized stiffness tensor $a_{ijkl}$ but obviates the need for introducing two additional angles needed to define the orientations of $\mathbf{k}^R$ and $\mathbf{k}^I$.

### B1 Real and imaginary parts of the wave vector

We start with the Christoffel equation in the perturbed medium:

$$(G_{ik} - \delta_{ik})\, g_k = 0\,, \tag{B1}$$

where $G_{ik} = a_{ijkl}\, p_j\, p_l$ is the Christoffel matrix, $\mathbf{p}$ is the complex slowness vector, and $\mathbf{g}$ is the polarization vector of the plane wave. Perturbation of equation B1 yields

$$\left(G^0_{ik} + \Delta G_{ik} - \delta_{ik}\right)\left(g^0_k + \Delta g_k\right) = 0\,, \tag{B2}$$

which can be linearized to obtain

$$\left(G^0_{ik} - \delta_{ik}\right)\Delta g_k + \Delta G_{ik}\, g^0_k = 0\,, \tag{B3}$$

where $\mathbf{g}^0$ is the plane-wave polarization in the background and $\Delta\mathbf{g}$ is the perturbation of the polarization vector. The polarization $\mathbf{g}^0$ defines whether the wave mode is P, SV, or SH. The mode obtained by perturbing the SV-wave will be denoted $S_1$, and the perturbed SH-wave will be denoted $S_2$. Multiplying equation B3 with $g^0_i$ (Jech & Pšenčík, 1989) reduces equation B3 to

$$\Delta G_{ik}\, g^0_i\, g^0_k = 0\,, \tag{B4}$$

with

$$\Delta G_{ik} = \Delta a_{ijkl}\, p^0_j\, p^0_l + 2a^0_{ijkl}\, \Delta p_j\, p^0_l\,, \tag{B5}$$

where $a^0_{ijkl}$ and $\mathbf{p}^0$ are defined in the isotropic background, and $\Delta a_{ijkl}$ and $\Delta\mathbf{p}$ are the perturbations. The tensors $a^0_{ijkl}$ and $\Delta a_{ijkl}$ are given by

$$a^0_{ijkl} = a^{R,0}_{ijkl} + i a^{I,0}_{ijkl} = a^{R,0}_{ijkl}\left(1 + \frac{i}{Q^0_{ijkl}}\right), \tag{B6}$$

$$\Delta a_{ijkl} = \Delta a^R_{ijkl} + i\Delta a^I_{ijkl}\,, \tag{B7}$$

where the superscripts "$R$" and "$I$" denote the real and imaginary parts, and $Q^0_{ijkl}$ is the ratio $a^R_{ijkl}/a^I_{ijkl}$. The background slowness $\mathbf{p}^0$ and its perturbation $\Delta\mathbf{p}$ can be expressed as

$$\mathbf{p}^0 = \left[-ip^{I,0}\sin\xi,\ 0,\ p^{R,0} - ip^{I,0}\cos\xi\right], \tag{B8}$$

$$\Delta\mathbf{p} = \left[-i\Delta p^I \sin\xi,\ 0,\ \Delta p^R - i\Delta p^I\cos\xi\right], \tag{B9}$$

where $p^{R,0}$, $p^{I,0}$ and $\Delta p^R$, $\Delta p^I$ are the magnitudes of the real and imaginary parts of $\mathbf{p}^0$ and $\Delta\mathbf{p}$, respectively.

Assuming $(Q^0\cos\xi) \gg 1$, we solve equation B4 for $\Delta k^R = \omega\Delta p^R$ and $\Delta k^I = \omega\Delta p^I$:

$$\frac{\Delta k^R}{k^{R,0}} = -\frac{\chi^R}{2} - \frac{\chi^I}{2Q^0}\left(1 - \frac{\sec^2\xi}{2}\right), \tag{B10}$$

$$\frac{\Delta k^I}{k^{I,0}} = -\frac{\chi^R}{2} + Q^0\chi^I, \tag{B11}$$

where $\chi^R$ and $\chi^I$ are the real and imaginary parts of $\chi = \Delta a_{ijkl} p^0_j p^0_l g^0_i g^0_k$. The above analysis is valid for all three modes (P-, $S_1$-, and $S_2$-waves). By choosing the corresponding $\mathbf{k}^0$ and $\chi$, we can compute the perturbations of the complex wave vector for any of the three modes. The term $\chi$ for P-, $S_1$-, and $S_2$-waves has the form

$$\begin{aligned}\chi_P =& \frac{1}{V^2_{P0}}\left(\Delta a^R_{33} + \frac{\Delta a^I_{33}}{Q_{P0}} + \frac{2\Delta a^I_{35}}{Q_{P0}}\tan\xi\right)\\ &+ i\,\frac{1}{V^2_{P0}}\left(-\frac{\Delta a^R_{33}}{Q_{P0}} + \Delta a^I_{33} - \frac{2\Delta a^R_{35}}{Q_{P0}}\tan\xi\right),\end{aligned} \tag{B12}$$

$$\begin{aligned}\chi_{S_1} =& \frac{1}{V^2_{S0}}\left(\Delta a^R_{55} + \frac{\Delta a^I_{55}}{Q_{S0}} + \frac{\Delta a^I_{15} - \Delta a^I_{35}}{Q_{S0}}\tan\xi\right)\\ &+ i\,\frac{1}{V^2_{S0}}\left(-\frac{\Delta a^R_{55}}{Q_{S0}} + \Delta a^I_{55} - \frac{\Delta a^R_{15} - \Delta a^R_{35}}{Q_{S0}}\tan\xi\right),\end{aligned} \tag{B13}$$

and

$$\begin{aligned}\chi_{S_2} =& \frac{1}{V^2_{S0}}\left(\Delta a^R_{44} + \frac{\Delta a^I_{44}}{Q_{S0}} + \frac{\Delta a^I_{46}}{Q_{S0}}\tan\xi\right)\\ &+ i\,\frac{1}{V^2_{S0}}\left(-\frac{\Delta a^R_{44}}{Q_{S0}} + \Delta a^I_{44} - \frac{\Delta a^R_{46}}{Q_{S0}}\tan\xi\right);\end{aligned} \tag{B14}$$

$Q_{P0}$ and $Q_{S0}$ are the P- and S-wave quality factors in the background medium. Substituting equations B12–B14 into equations B10 and B11 and retaining only the terms linear in $\Delta a_{ij}$ yields

$$\begin{aligned}\frac{\Delta k^R_P}{k^{R,0}_P} \approx& -\frac{1}{V^2_{P0}}\left[\frac{\Delta a^R_{33}}{2} + \frac{\Delta a^I_{33}}{Q_{P0}}\left(1 - \frac{\sec^2\xi}{4}\right)\right.\\ &\left. + \frac{\Delta a^I_{35}}{Q_{P0}}\tan\xi\right],\end{aligned} \tag{B15}$$

$$\frac{\Delta k_P^I}{k_P^{I,0}} \approx -\frac{1}{V_{P0}^2}\left(\frac{3\Delta a_{33}^R}{2} - Q_{P0}\Delta a_{33}^I + 2\Delta a_{35}^R \tan\xi\right), \tag{B16}$$

$$\frac{\Delta k_{S_1}^R}{k_{S_1}^{R,0}} \approx -\frac{1}{V_{S0}^2}\left[\frac{\Delta a_{55}^R}{2} + \frac{\Delta a_{55}^I}{Q_{S0}}\left(1 - \frac{\sec^2\xi}{4}\right) + \frac{\Delta a_{15}^I - \Delta a_{35}^I}{2Q_{S0}}\tan\xi\right], \tag{B17}$$

$$\frac{\Delta k_{S_1}^I}{k_{S_1}^{I,0}} \approx -\frac{1}{V_{S0}^2}\left(\frac{3\Delta a_{55}^R}{2} - Q_{S0}\Delta a_{55}^I + (\Delta a_{15}^R - \Delta a_{35}^R)\tan\xi\right), \tag{B18}$$

$$\frac{\Delta k_{S_2}^R}{k_{S_2}^{R,0}} \approx -\frac{1}{V_{S0}^2}\left[\frac{\Delta a_{44}^R}{2} + \frac{\Delta a_{44}^I}{Q_{S0}}\left(1 - \frac{\sec^2\xi}{4}\right) + \frac{\Delta a_{46}^I}{2Q_{S0}}\tan\xi\right], \tag{B19}$$

and

$$\frac{\Delta k_{S_2}^I}{k_{S_2}^{I,0}} \approx -\frac{1}{V_{S0}^2}\left(\frac{3\Delta a_{44}^R}{2} - Q_{S0}\Delta a_{44}^I + \Delta a_{46}^R \tan\xi\right). \tag{B20}$$

### B2 Normalized phase attenuation coefficient

We linearize the normalized phase attenuation coefficient $\mathcal{A}$ for $\xi = 0^\circ$ by retaining only the first-order terms:

$$\mathcal{A}|_{\xi=0^\circ} = \left.\frac{k^I}{k^R}\right|_{\xi=0^\circ} = \left.\frac{k^{I,0} + \Delta k^I}{k^{R,0} + \Delta k^R}\right|_{\xi=0^\circ} \tag{B21}$$

$$= \frac{1}{2Q_0}\left(1 + \frac{\Delta k^I}{k^{I,0}} - \frac{\Delta k^R}{k^{R,0}}\right). \tag{B22}$$

By substituting $\Delta k^R$ and $\Delta k^I$ from equations B15–B20 into equation B22, we obtain $\mathcal{A}|_{\xi=0^\circ}$ in arbitrarily anisotropic media for all three modes:

$$\mathcal{A}|_{\xi=0^\circ,P} = \frac{1}{2Q_{P0}} - \frac{1}{2V_{P0}^2}\left(\frac{\Delta a_{33}^R}{Q_{P0}} - \Delta a_{33}^I\right), \tag{B23}$$

$$\mathcal{A}|_{\xi=0^\circ,S_1} = \frac{1}{2Q_{S0}} - \frac{1}{2V_{S0}^2}\left(\frac{\Delta a_{55}^R}{Q_{S0}} - \Delta a_{55}^I\right), \tag{B24}$$

$$\mathcal{A}|_{\xi=0^\circ,S_2} = \frac{1}{2Q_{S0}} - \frac{1}{2V_{S0}^2}\left(\frac{\Delta a_{44}^R}{Q_{S0}} - \Delta a_{44}^I\right). \tag{B25}$$

### B3 Normalized group attenuation coefficient

To obtain the normalized group attenuation from equation 32, we find the quantity $\tan\psi\cos\phi = V_{g1}/V_{g3}$ from equation A16:

$$\tan\psi_P \cos\phi_P = \frac{2\Delta a_{35}^R}{V_{P0}^2}, \tag{B26}$$

$$\tan\psi_{S_1} \cos\phi_{S_1} = \frac{\Delta a_{15}^R - \Delta a_{35}^R}{V_{S0}^2}, \tag{B27}$$

and

$$\tan\psi_{S_2} \cos\phi_{S_2} = \frac{\Delta a_{46}^R}{V_{S0}^2}, \tag{B28}$$

where only the leading-order terms are retained.

Next, we substitute $\Delta k^R$ and $\Delta k^I$ from equations B15–B20 and $\tan\psi$ from equations B26–B28 into equation 32 and retain only the terms linear in $\Delta a_{ij}$:

$$\mathcal{A}_{g,P} = \frac{1}{2Q_{P0}} - \frac{1}{2V_{P0}^2}\left(\frac{\Delta a_{33}^R}{Q_{P0}} - \Delta a_{33}^I\right), \tag{B29}$$

$$\mathcal{A}_{g,S_1} = \frac{1}{2Q_{S0}} - \frac{1}{2V_{S0}^2}\left(\frac{\Delta a_{55}^R}{Q_{S0}} - \Delta a_{55}^I\right), \tag{B30}$$

and

$$\mathcal{A}_{g,S_2} = \frac{1}{2Q_{S0}} - \frac{1}{2V_{S0}^2}\left(\frac{\Delta a_{44}^R}{Q_{S0}} - \Delta a_{44}^I\right). \tag{B31}$$

## APPENDIX C: SHEAR-WAVE PHASE AND GROUP QUANTITIES IN TI MEDIA

Here, we present closed-form expressions for the shear-wave parameters $\Delta k^R$, $\Delta k^I$, $\mathcal{A}$, and $\mathcal{A}_g$ in TI media. Note that all equations in Appendix A are derived for the coordinate frame defined by the vectors $\mathbf{k}^R$ and $\mathbf{k}^I$. Therefore, in order to obtain $\Delta k^R$, $\Delta k^I$, $\mathcal{A}$, and $\mathcal{A}_g$ as a function of the phase angle $\theta$ (the angle between $\mathbf{k}^R$ and the $x_3$-axis), one needs to rotate the tensor $\Delta a_{ijkl}$ accordingly. Since $\mathbf{k}^I$ is assumed to lie in the plane defined by $\mathbf{k}^R$, $\Delta a_{ijkl}$ in Appendix A is rotated by the phase angle $\theta$ around the $x_2$-axis.

By linearizing the rotated tensor $\Delta a_{ijkl}$ in the Thomsen velocity-anisotropy parameters $\epsilon$, $\delta$, and $\gamma$ and in the Thomsen-style attenuation-anisotropy parameters $\epsilon_Q$, $\delta_Q$, and $\gamma_Q$ (Zhu & Tsvankin, 2006), we obtain the real ($\mathbf{k}^R$) and imaginary ($\mathbf{k}^I$) parts of the wave vector from equations B17–B20:

$$\frac{\Delta k_{SV}^R}{k_{SV}^{R,0}} = -\sigma \sin^2\theta\cos^2\theta, \tag{C1}$$

$$\frac{\Delta k^I_{SV}}{k^{I,0}_{SV}} = (\epsilon_Q - \delta_Q)\frac{g^2}{g_Q}\sin^2\theta\cos^2\theta + \sigma\frac{2-3g_Q}{g_Q}\sin^2\theta\cos^2\theta - \sigma\sin 2\theta\cos 2\theta\tan\xi\,, \tag{C2}$$

$$\frac{\Delta k^R_{SH}}{k^{R,0}_{SH}} = -\gamma\sin^2\theta\,, \tag{C3}$$

$$\frac{\Delta k^I_{SH}}{k^{I,0}_{SH}} = \gamma_Q\sin^2\theta - \gamma\sin^2\theta - \gamma\sin 2\theta\tan\xi\,, \tag{C4}$$

where $g = V_{P0}/V_{S0}$, the parameter $\sigma = g^2(\epsilon-\delta)$ controls the SV-wave phase velocity, $g_Q = Q_{P0}/Q_{S0}$, and the parameters $\gamma$ and $\gamma_Q$ are responsible for the SH-wave velocity and attenuation anisotropy, respectively (Zhu & Tsvankin, 2006).

The normalized SV- and SH-wave phase attenuation coefficients for $\xi = 0^\circ$ can be found from equations B24 and B25:

$$\mathcal{A}|_{\xi=0^\circ,SV} = \frac{1}{2Q_{S0}}\left(1+\sigma_Q\sin^2\theta\cos^2\theta\right), \tag{C5}$$

$$\mathcal{A}|_{\xi=0^\circ,SH} = \frac{1}{2Q_{S0}}\left(1+\gamma_Q\sin^2\theta\right), \tag{C6}$$

where the parameter $\sigma_Q$ (Zhu & Tsvankin, 2006) controls the SV-wave attenuation coefficient:

$$\sigma_Q = \frac{1}{g_Q}\left[2\sigma(1-g_Q) + g^2(\epsilon_Q-\delta_Q)\right]. \tag{C7}$$

To obtain the linearized shear-wave group angles in TI media, we use equations B27 and B28 (see also Tsvankin, 2005):

$$\tan\psi_{SV}\cos\phi_{SV} = \sigma\sin 2\theta\cos 2\theta \tag{C8}$$

and

$$\tan\psi_{SH}\cos\phi_{SH} = \gamma\sin 2\theta\,. \tag{C9}$$

Substituting the anisotropy parameters into equations B30 and B31 yields the following group attenuation coefficients:

$$\mathcal{A}_{g,SV} = \frac{1}{2Q_{S0}}\left(1+\sigma_Q\sin^2\theta\cos^2\theta\right), \tag{C10}$$

$$\mathcal{A}_{g,SH} = \frac{1}{2Q_{S0}}\left(1+\gamma_Q\sin^2\theta\right). \tag{C11}$$

## APPENDIX D: ATTENUATION FOR LARGE INHOMOGENEITY ANGLES

Here, we develop closed-form expressions for the wave vector $\mathbf{k}$ and group attenuation coefficient $\mathcal{A}_g$ for large angles $\xi$. For simplicity, we analyze only $S_2$-waves; expressions for P- and $S_1$-waves can be derived using the same procedure. The development follows the same approach as that described in Appendix B. The group angle $\psi^0$ in the background, however, does not vanish (equation 26), and the background vector $\mathbf{k}^0 = \mathbf{k}^{R,0} - i\mathbf{k}^{I,0}$ is given by equations 23 and 24. (Note that for small and moderate angles $\xi$ considered in Appendix B, the group angle $\psi^0$ was zero.) For large $\xi$, the real ($k^{R,0}$) and imaginary ($k^{I,0}$) parts of the background wave vector are related by (equation 25)

$$\frac{k^{I,0}}{k^{R,0}} = 1 - Q^0\cos\xi\,, \tag{D1}$$

and the group angle $\psi^0$ is expressed as (equation 26)

$$\tan\psi^0 = \frac{1}{Q^0} - \cos\xi\,, \tag{D2}$$

where $Q^0$ is the background quality factor. The perturbation produces a change in both the wave vector ($\Delta k^R - i\Delta k^I$) and the group direction.

First, we obtain $k^R$ and $k^I$ by solving equation B4 and linearizing the result in $\Delta a_{ij}$. Eliminating terms quadratic or higher-order in $Q^0\cos\xi$ and those proportional to $\Delta a_{ij}Q^0\cos\xi$, as well as setting terms quadratic in $\sin\xi$ to one, we find

$$\frac{k^R_{S_2}}{k^{R,0}_{S_2}} = \frac{k^I_{S_2}}{k^{I,0}_{S_2}} = 1 - \frac{1}{2V^2_{S0}}\left(\Delta a^R_{46} + \frac{\Delta a^I_{46}}{Q_{S0}}\right)\tan\xi + \frac{1}{4V^2_{S0}\cos\xi}\left(\Delta a^I_{44} - \frac{\Delta a^R_{44}}{Q_{S0}} - \Delta a^I_{66} + \frac{\Delta a^R_{66}}{Q_{S0}}\right). \tag{D3}$$

For the special case of TI media, the $S_2$-mode becomes the SH-wave, and equation D3 (after eliminating terms proportional to $\gamma/Q^2_{S0}$ and $\gamma_Q/Q^2_{S0}$) takes the form

$$\frac{k^R_{S_2}}{k^{R,0}_{S_2}} = \frac{k^I_{S_2}}{k^{I,0}_{S_2}} \approx 1 + \frac{\gamma\sin 2\theta}{2}\tan\xi - \frac{\gamma_Q\cos 2\theta}{4Q_{S0}}\frac{1}{\cos\xi}\,. \tag{D4}$$

The product $\tan\psi\cos\phi$ needed to find $\mathcal{A}_g$ can be obtained from equation A16:

$$\tan\psi\cos\phi = \frac{1}{Q_{S0}} - \cos\xi - \frac{1}{4V^2_{S0}}\left[\frac{2\Delta a^I_{46}}{Q_{S0}} - 6\Delta a^R_{46} + \left(\frac{3\Delta a^R_{44}}{Q_{S0}} + \frac{\Delta a^R_{66}}{Q_{S0}} + \Delta a^I_{44} - 5\Delta a^I_{66}\right)\sin\xi\right]. \tag{D5}$$

The group attenuation coefficient $\mathcal{A}_g$ is found by

substituting equations D1–D5 into equation 31:

$$\mathcal{A}_g = \frac{1}{Q_{S0}} - \cos\xi$$

$$- \frac{1}{4V_{S0}^2}\left[\frac{3\Delta a_{44}^R}{Q_{S0}} + \frac{\Delta a_{66}^R}{Q_{S0}} + \Delta a_{44}^I - 5\Delta a_{66}^I\right.$$

$$\left. + \left(\frac{2\Delta a_{46}^I}{Q_{S0}} - 6\Delta a_{46}^R\right)\sin\xi\right]; \qquad \text{(D6)}$$

equation D6 is linearized in $\Delta a_{ij}$ and $(Q_{S0}\cos\xi)$, and terms proportional to $(\Delta a_{ij} Q_{S0}\cos\xi)$ have been eliminated. The range of $\xi$ for which equation D6 is valid is set by the assumption $Q_{S0}\cos\xi \ll 1$ which ensures that $\mathcal{A}_g$ is positive. For the special case of TI media, $\mathcal{A}_g$ takes a simpler form after linearization in the anisotropy parameters:

$$\mathcal{A}_g = \frac{1}{Q_{S0}} - \cos\xi - \frac{3\gamma\sin 2\theta}{2}\sin\xi$$

$$+ \frac{2\gamma\cos 2\theta}{Q_{S0}} + \frac{\gamma_Q\cos 2\theta}{4Q_{S0}} + \frac{\gamma_Q\cos^2\theta}{4Q_{S0}}\,. \qquad \text{(D7)}$$